Supplementary Information

Supramolecular Self-Assemblies of Ru(II) Phototherapeutics: Biological Activity of Micro- and Nano-particles Acting as Reservoirs

Jérôme Laisney[b†] and Sarah M. Kriger,[a†] Dmytro Havrylyuk,[a] Jason M. Unrine,[c] David K. Heidary,[a] and Edith C. Glazer [a*]

[a] Department of Chemistry, North Carolina State University, 2620 Yarbrough Dr., Raleigh, NC, 27607
[b] Department of Chemistry, University of Kentucky, 505 Rose St., Lexington, KY 40506
[c] Department of Plant and Soil Science, University of Kentucky, Lexington, KY 40546, USA
[†] Authors contributed equally
* To whom correspondence may be addressed: eglazer@ncsu.edu

Table of Contents:

Figure S15. TEM, HAADF and elemental mapping of the **380 nm PVP** $[Ru(bpy)_2(dmbpy)](PF_6)_2$ nanoparticles prepared by fast precipitation at room temperature in the presence of PVP55 confining agent.
Figure S16. TEM, HAADF and elemental mapping of the **300 nm PEG** $[Ru(bpy)_2(dmbpy)](PF_6)_2$ nanoparticles prepared by fast precipitation at room temperature in the presence of PEG6000 confining agent.
Figure S17. Chemical structures of polymers used in this study.
Figure S18. UV-Visible spectra as function of time of $[Ru(bpy)_3](PF_6)_2$ and $[Ru(bpy)_2(dmbpy)](PF_6)_2$ solubilized complex in methanol dialyzed in water at 37°C in the dark.
Figure S19. UV-Visible spectra as function of time of $[Ru(bpy)_3](PF_6)_2$ particle suspensions dialyzed in water at 37°C in the dark or after light activation.
Figure S20. UV-Visible spectra as function of time of $[Ru(bpy)_2(dmbpy)](PF_6)_2$ particles suspension dialyzed in water at 37°C in the dark or after light activation.
Figure S21. Excitation-emission properties of the $[Ru(bpy)_3)]Cl_2$ complex in water and at different concentration.
Figure S22. Excitation-emission properties of the $[Ru(bpy)_3](PF_6)_2$ particles compared to the solubilized complex (Cl form) in water (10 µM suspensions).
Figure S23. Cytotoxicity dose responses of compound **1** and associated particles in HL60 cells.
Figure S24. Cytotoxicity dose responses of compound **1** and associated particles in HeLa cells.
Figure S25. Cytotoxicity dose responses of compound **1** and associated particles in A549 cells.
Figure S26. Cytotoxicity dose responses of compound **2** soluble complex with 24, 48, and 72 hour incubation following indigo light irradiation for 1 minute in HL60 cells.
Figure S27. Cell viability of HL60 cells treated with PVP and PEG polymers.
Figure S28. Cytotoxicity dose responses of compound **2** PF_6 and associated particles in HL60.
Figure S29. Cytotoxicity dose responses of compound **2** BF_4 and associated particles in HL60.
Figure S30. Cytotoxicity dose responses of **500 nm** compound **2** particles post-functionalized with positively charge PLR, PLK, and PLO polymer in HL60 cells.
Figure S31. Cytotoxicity dose responses of **3.8 µm** compound **2** particles post-functionalized with positively charge PLR, PLK, and PLO polymer in HL60 cells.
Figure S32. Cytotoxicity dose responses of **250 nm** compound **2** particles post-functionalized with positively charge PLR, PLK, and PLO polymer in HL60 cells.
Figure S33. Accumulation of Ru in A459 cells at 1, 16, and 24 hours for compound **1** and associated particles and the change in intracellular Ru content over time fitted with a linear regression.
Figure S34. Fluorescence localization microscopy of compound **1** particles.
Figure S35. Seahorse extracellular flux analysis and basal respiration of compound **1** in the absence of light and with 1 minute indigo light irradiation.
Figure S36. Seahorse extracellular flux analysis and basal respiration of compound **2** in the absence of light and with 1 minute indigo light irradiation.
Figure S37. DAB polymerization in A459 cells followed by light microscopy as function of the irradiation time in presence of the $[Ru(bpy)_3](PF_6)_2$ complex.
Figure S38. TEM, HAADF and EDS mapping (Os, O, P, F, Ru) of a 1.6 µm particle undergoing dissolution in A459 cells.
Figure S39. STEM images of A549 cells cross sections treated with compound 1 soluble complex and 40 nm PVP particles.
Figure S40. TEM and STEM images of A459 cell cross sections for cells untreated or treated with compound **1** and particles for 16 hours.
Figure S41. Cytotoxicity dose responses of compound **2** in HeLa cells.
Figure S42. Cytotoxicity dose responses of compound **1** and associated particles in HEK cells.

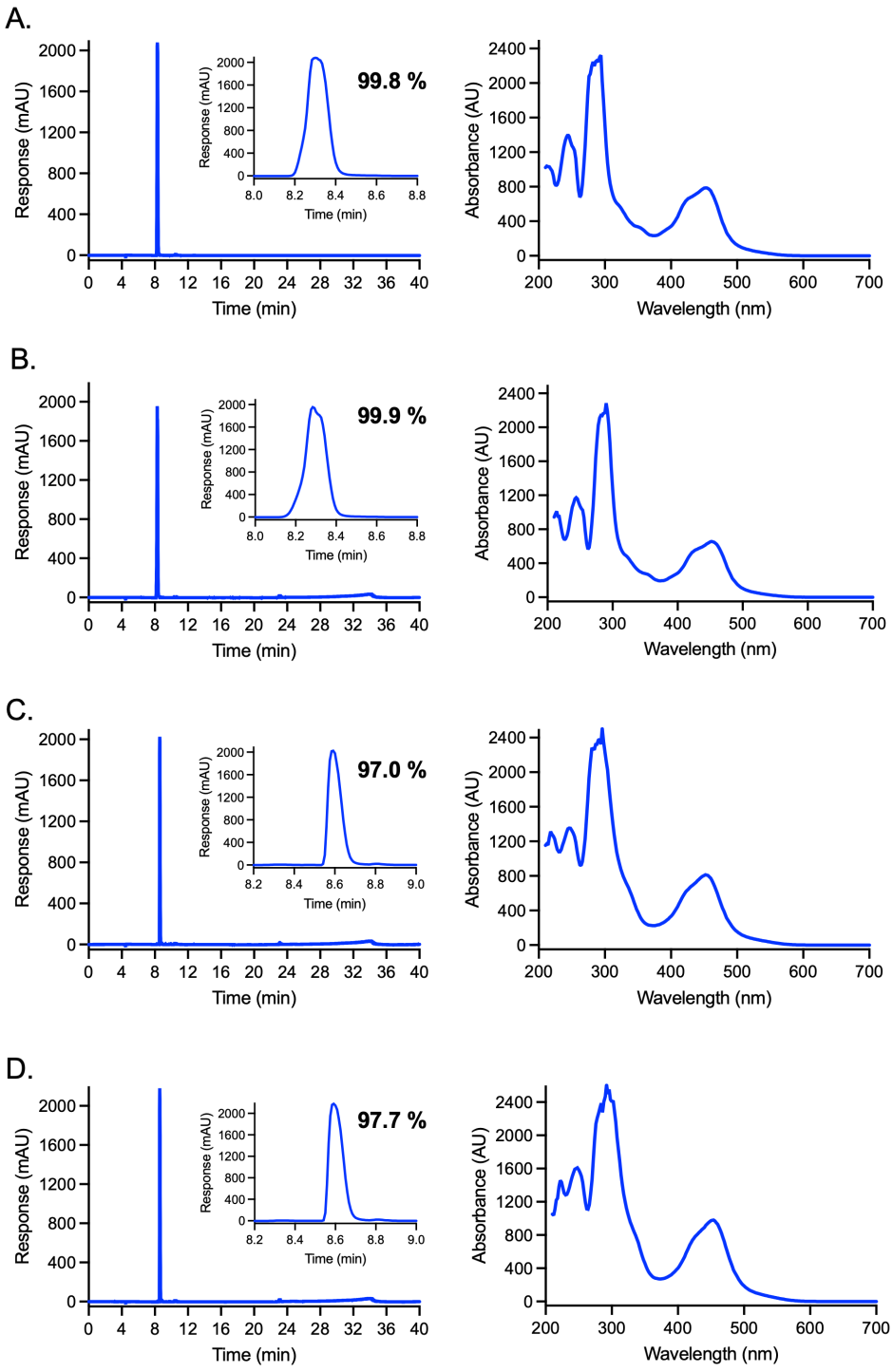

Figure S1. HPLC chromatograms of (A) $[Ru(bpy)_3](PF6)_2$, (B) $[Ru(bpy)_3](Cl)_2$, (C) $[Ru(bpy)_2(dmbpy)](PF_6)_2$ and (D) $[Ru(bpy)_2(dmbpy)](BF_4)_2$ stock compounds with a zoomed insert of the major peak (inlay), purity value as determined by % area, and extracted UV-Vis spectrum for the major peak (right).

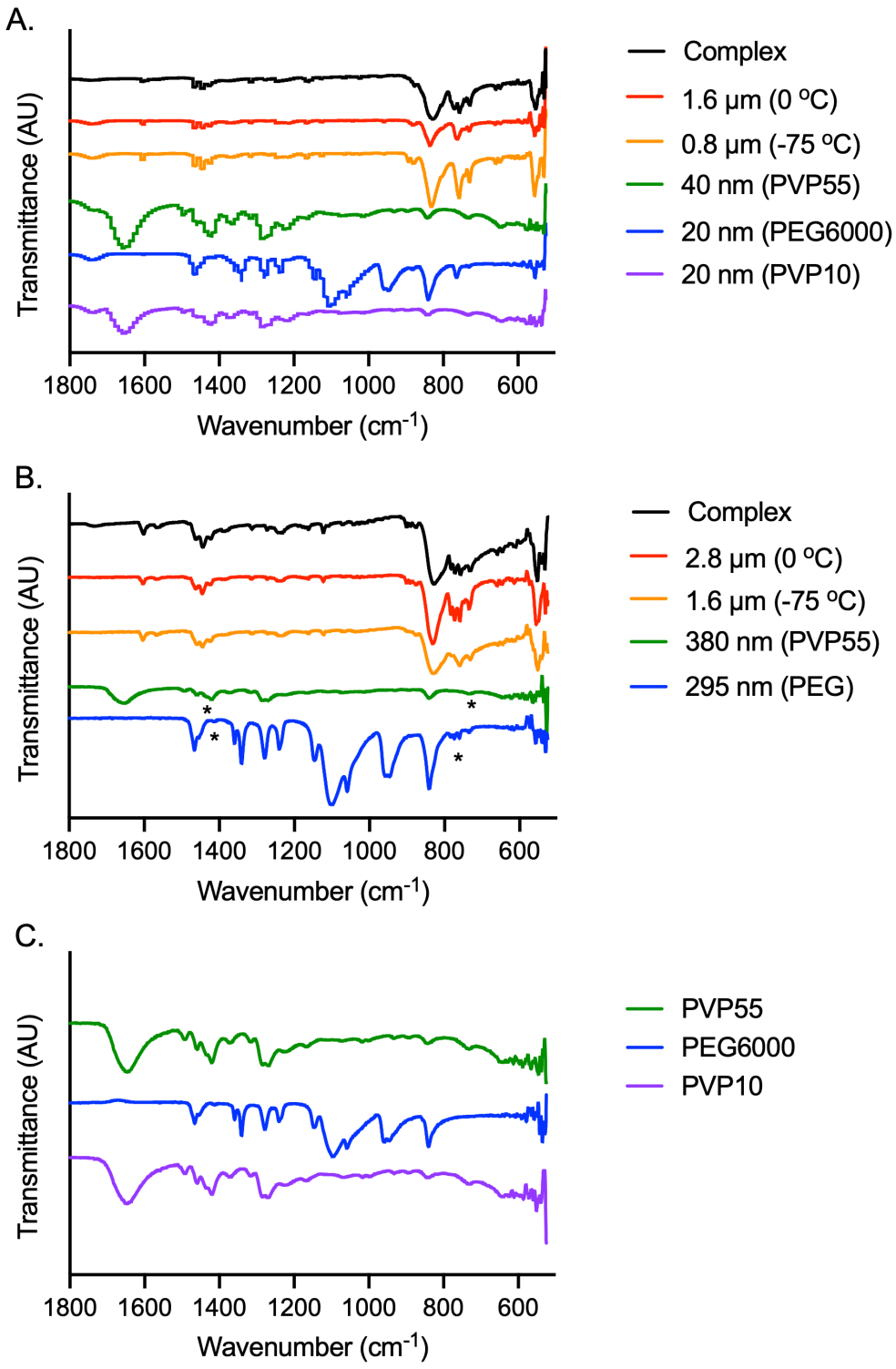

Figure S2. FTIR spectra in the low- and mid-IR range (600-1800 cm^{-1}) of the (A) $[Ru(bpy)_3](PF_6)_2$ complex and particles, (B) $[Ru(bpy)_2(dmbpy)](PF_6)_2$ complex and particles, and (C) confining polymers. (*) Characteristic peaks of the Ru complex in the nanocomposite spectra (5% Ru:polymer ratio).

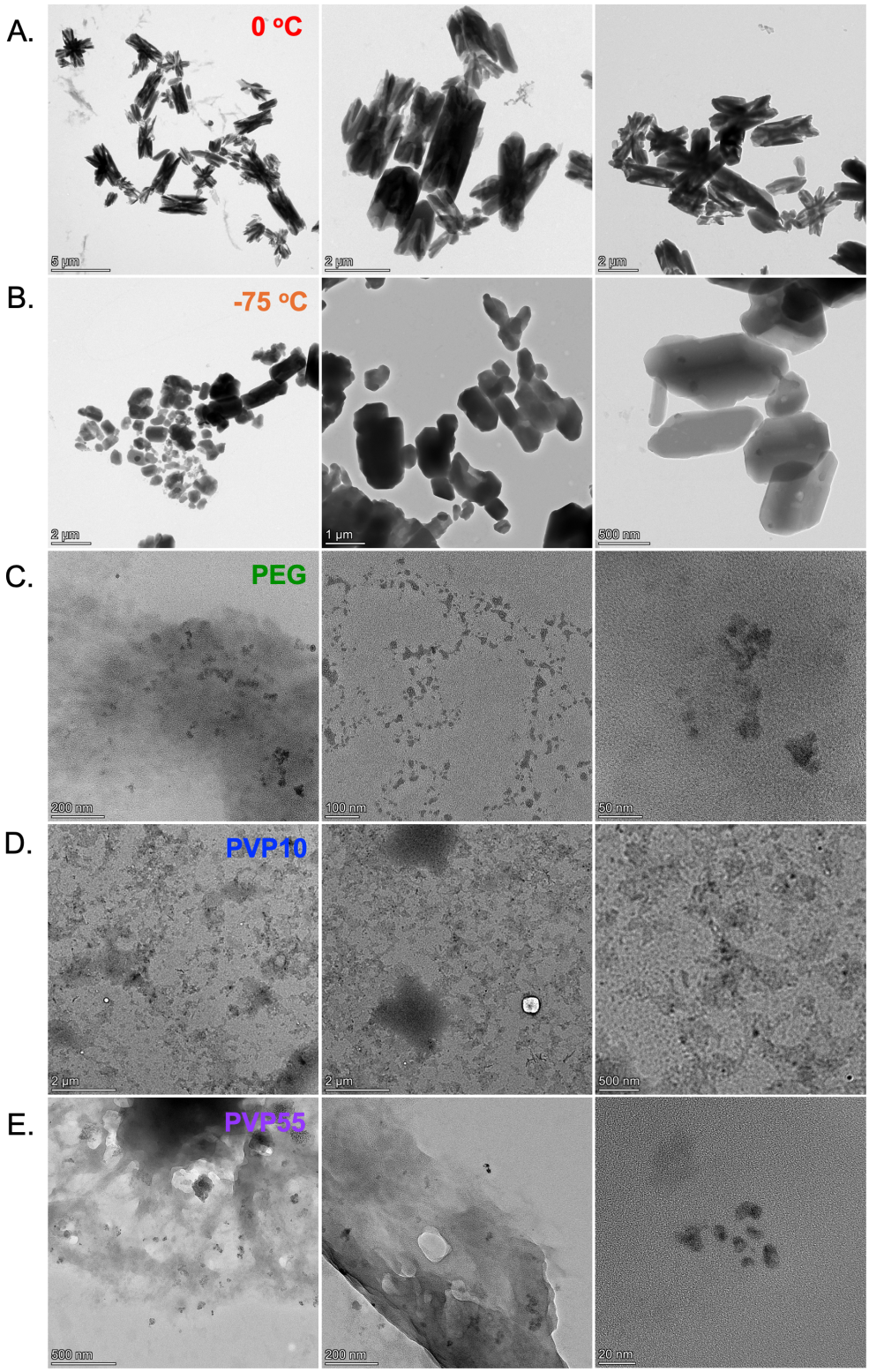

Figure S3. Transmission Electron Microscopy (TEM) of compound **1** particles prepared by fast precipitation. Particles formed at (A) 0 °C (1.6 µm), (B) -75 °C (0.8 µm), room temperature in presence of (C) PEG6000 (20 nm PEG), (D) PVP10 (40 nm PVP10) and (E) PVP55 (20 nm PVP55).

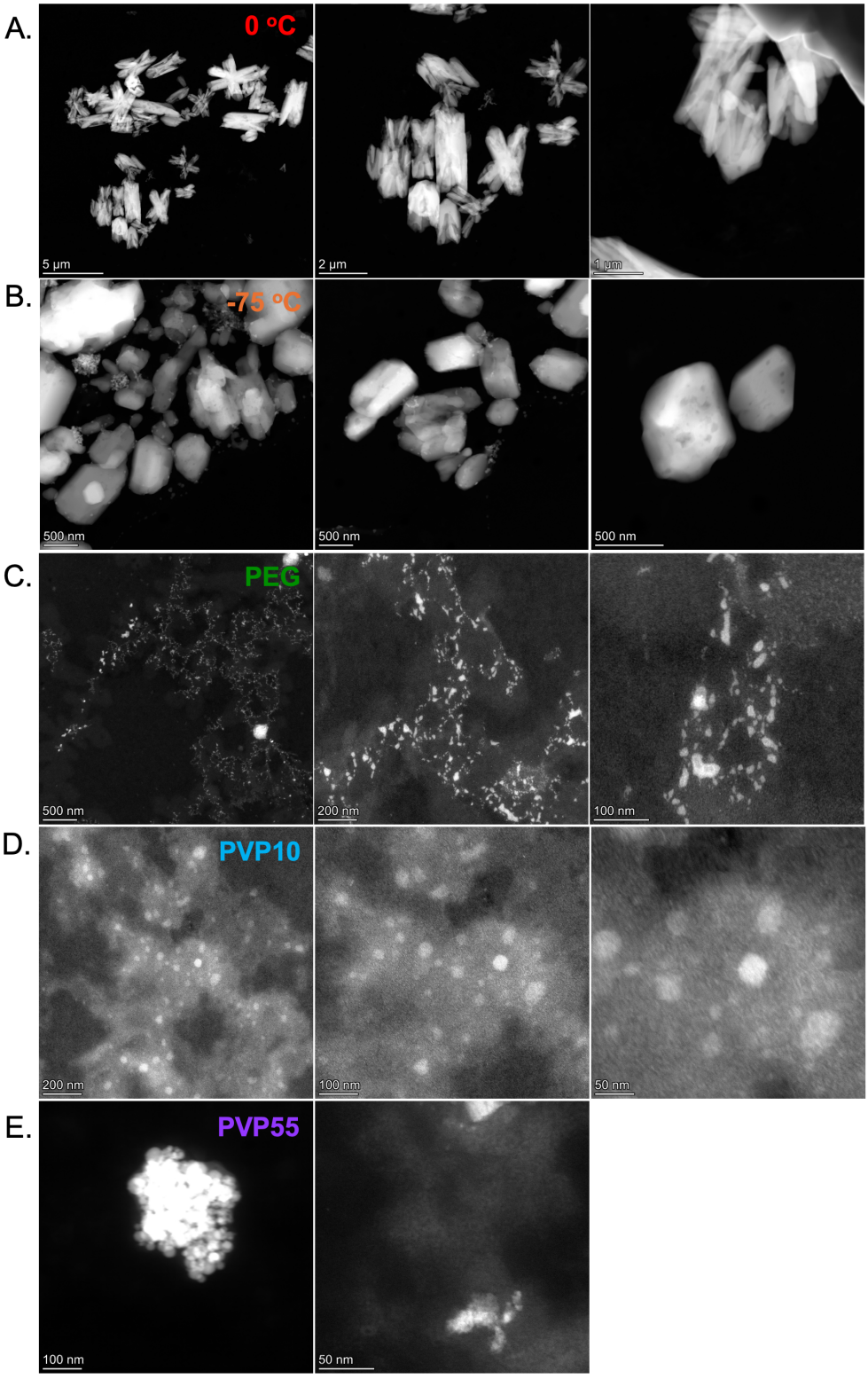

Figure S4. Scanning Transmission Electron Microscopy (STEM) of compound **1** particles prepared by fast precipitation. Particles formed at (A) 0 °C (1.6 µm), (B) -75 °C (0.8 µm), room temperature in presence of (C) PEG6000 (20 nm PEG), (D) PVP10 (40 nm PVP10) and (E) PVP55 (20 nm PVP55).

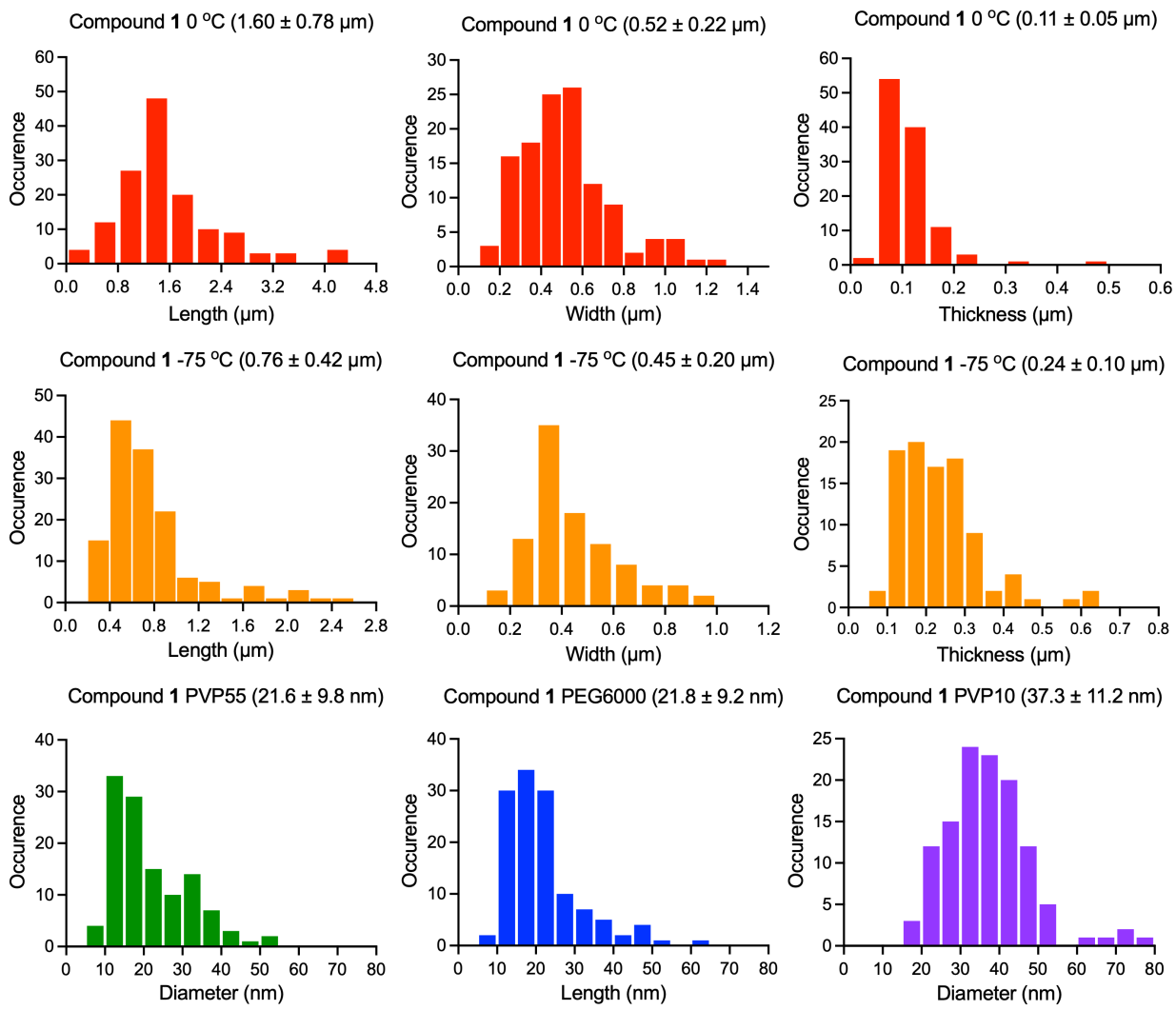

Figure S5. The size distribution of $[Ru(bpy)_3](PF6)_2$ particles. The statistics for size distribution were obtained by measuring the dimensions were obtained by measuring the dimensions (length, width, and thickness) on more than 100 objects.

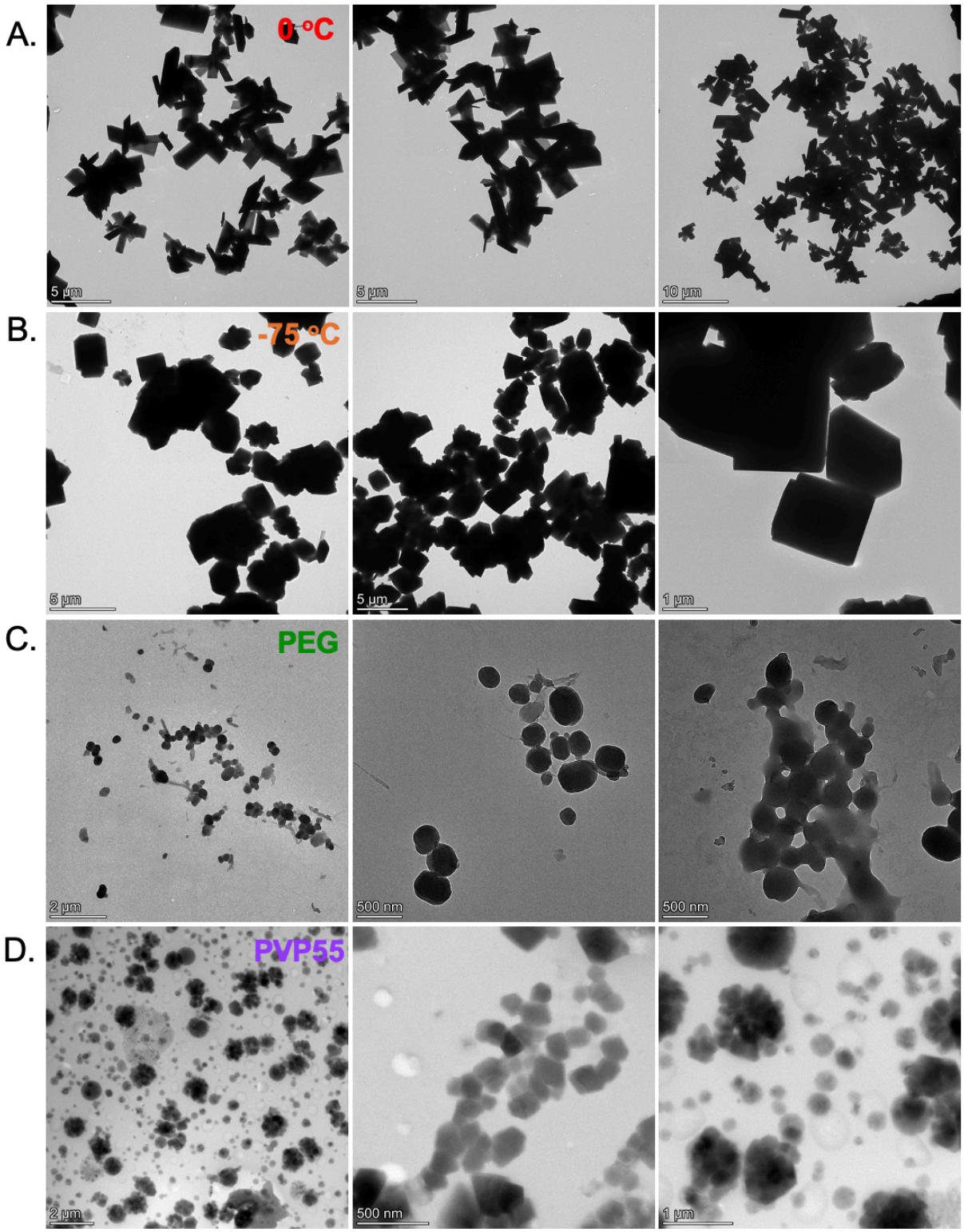

Figure S6. Transmission Electron Microscopy (TEM) of compound **2** particles prepared by fast precipitation. Particles formed at (A) 0 °C (2.8 µm), (B) -75 °C (1.6 µm), room temperature in presence of (C) PEG6000 (295 nm PEG), and (D) PVP55 (380 nm PVP55).

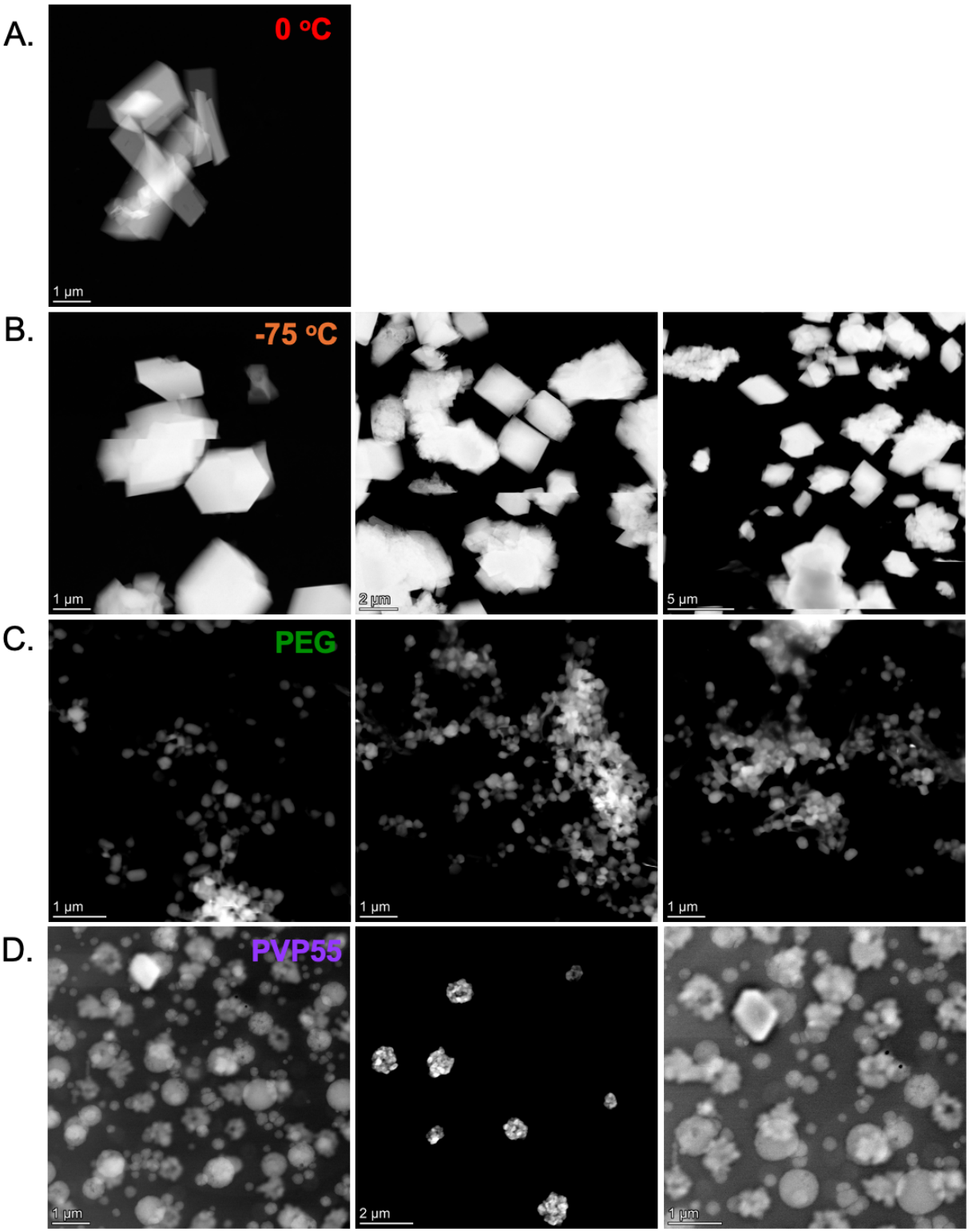

Figure S7. Scanning Transmission Electron Microscopy (STEM) of compound **2** particles prepared by fast precipitation. Particles formed at (A) 0 °C (2.8 µm), (B) -75 °C (1.6 µm), room temperature in presence of (C) PEG6000 (295 nm PEG), and (D) PVP55 (380 nm PVP55).

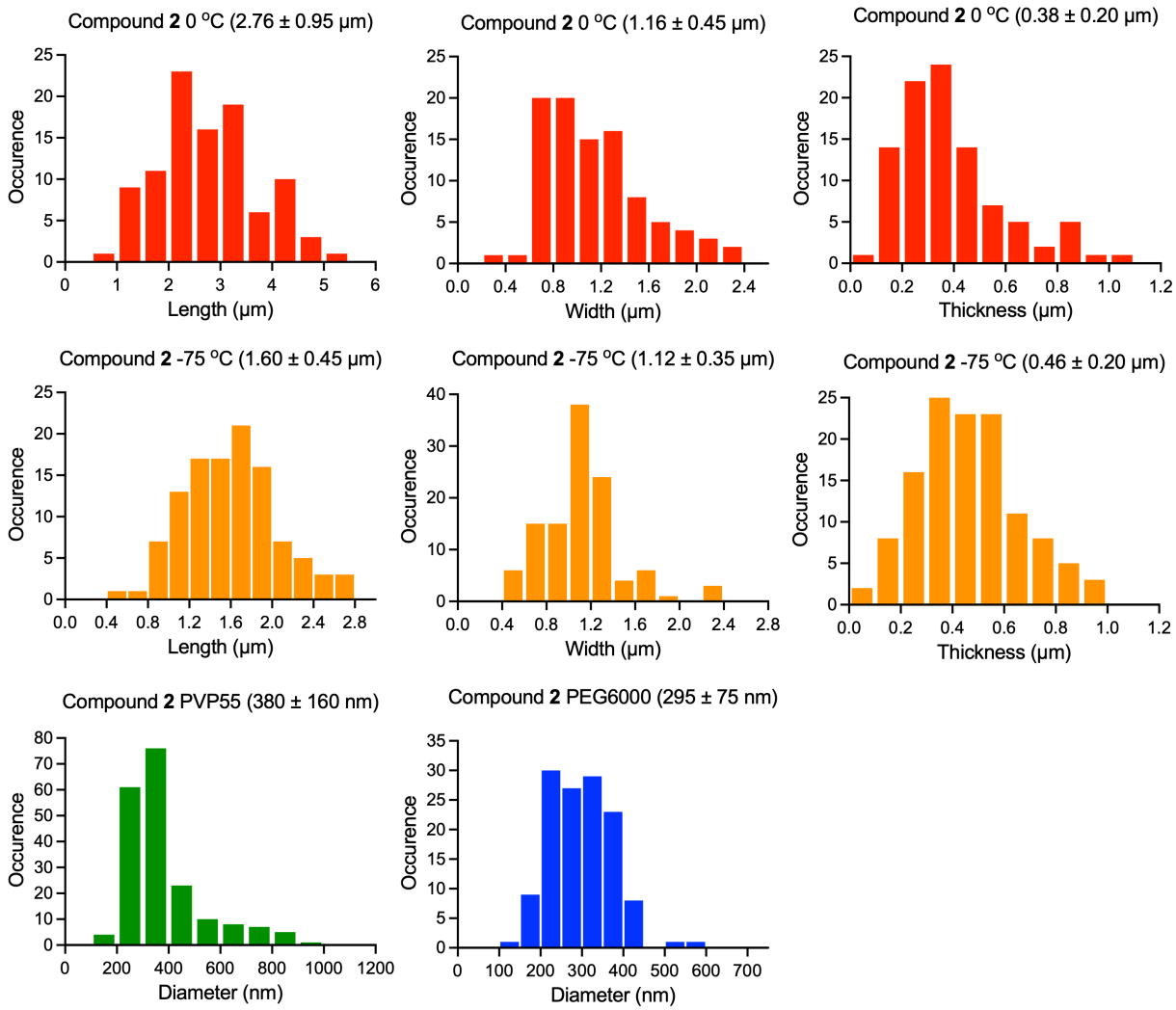

Figure S8. The size distribution of $[Ru(bpy)_2(dmbpy)](PF6)_2$ particles. The statistics for size distribution were obtained by measuring the dimensions were obtained by measuring the dimensions (length, width, and thickness) on more than 100 objects.

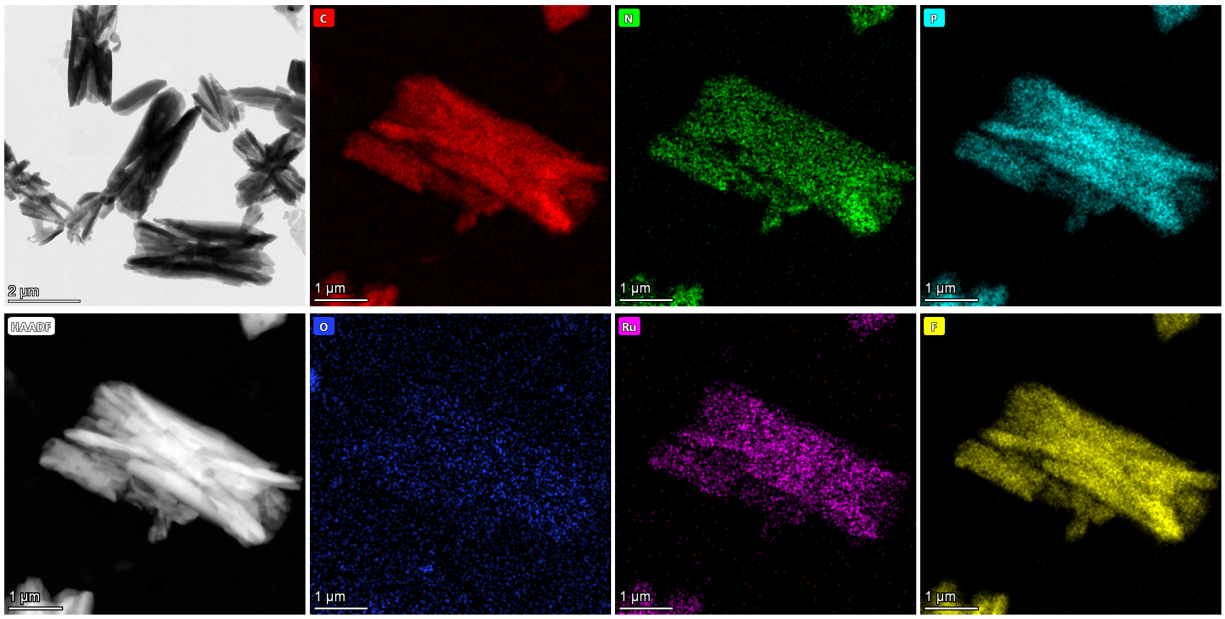

Figure S9. TEM, HAADF and elemental mapping (C-red, N-green, O-blue, P-cyan, F-yellow, Ru-pink) of the **1.6 µm** $[Ru(bpy)_3](PF_6)_2$ microparticles prepared by fast precipitation at 0 °C.

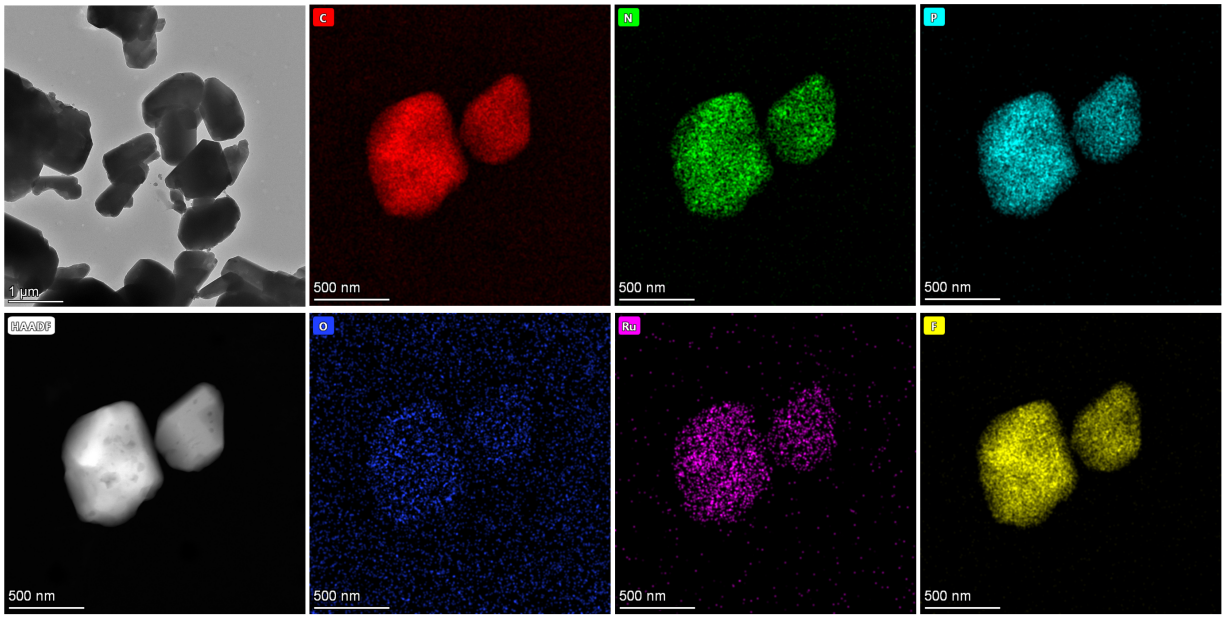

Figure S10. TEM, HAADF and elemental mapping (C-red, N-green, O-blue, P-cyan, F-yellow, Ru-pink) of the **0.8 µm** $[Ru(bpy)_3](PF_6)_2$ microparticles prepared by fast precipitation at -75 °C.

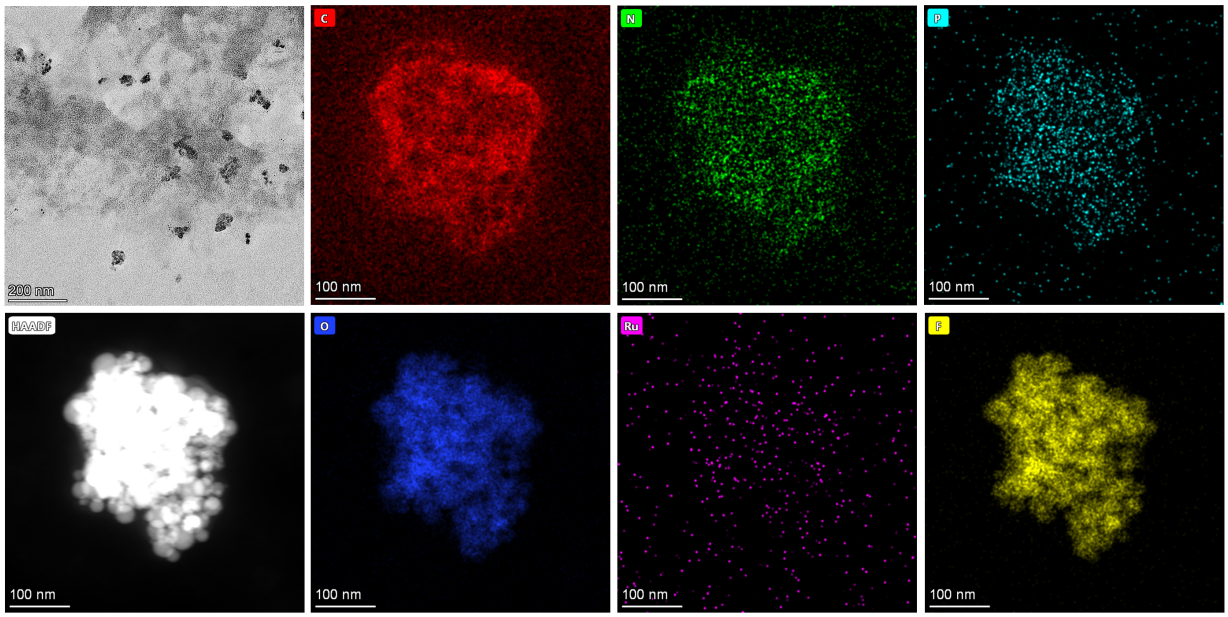

Figure S11. TEM, HAADF and elemental mapping (C-red, N-green, O-blue, P-cyan, F-yellow, Ru-pink) of the **40 nm PVP** $[Ru(bpy)_3](PF_6)_2$ nanoparticles prepared by fast precipitation at room temperature in the presence of PVP55 confining agent.

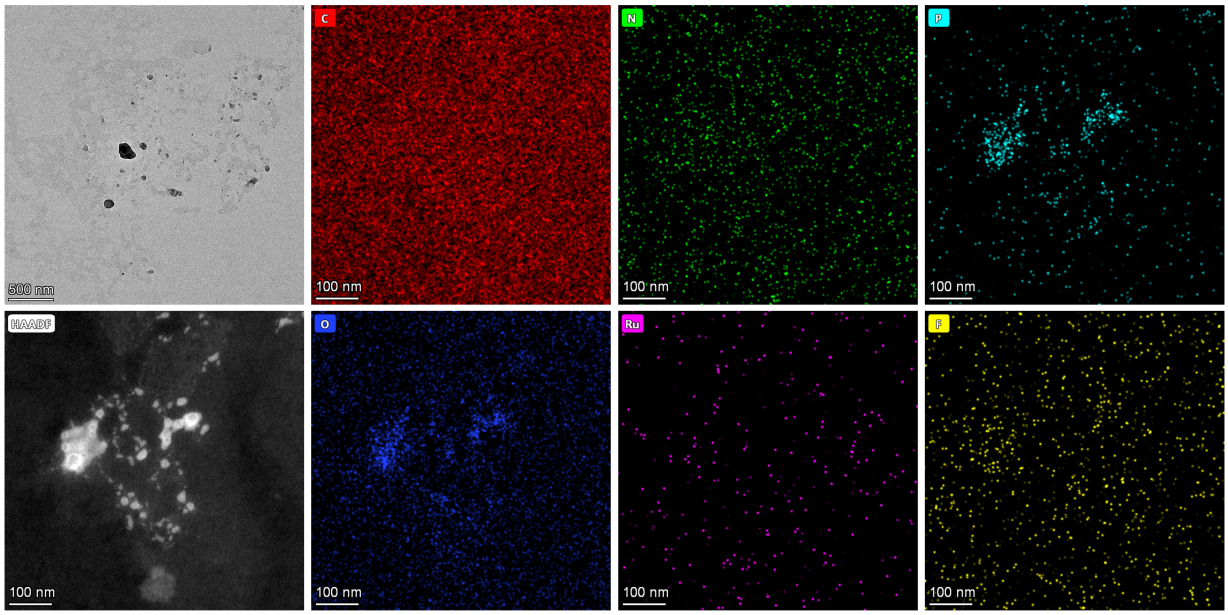

Figure S12. TEM, HAADF and elemental mapping (C-red, N-green, O-blue, P-cyan, F-yellow, Ru-pink) of the **20 nm PEG** $[Ru(bpy)_3](PF_6)_2$ nanoparticles prepared by fast precipitation at room temperature in the presence of PEG6000 confining agent.

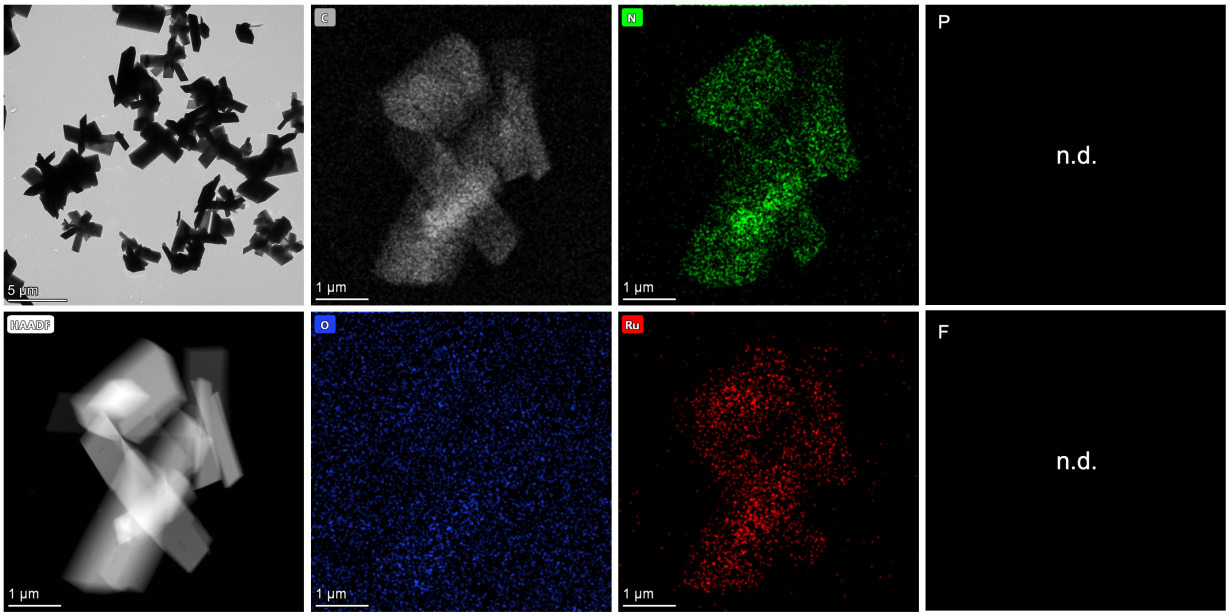

Figure S13. TEM, HAADF and elemental mapping (C-red, N-green, O-blue, P-cyan, F-yellow, Ru-pink) of the **3 µm** $[Ru(bpy)_2(dmbpy)](PF_6)_2$ microparticles prepared by fast precipitation at 0 °C (n.d. = not determined).

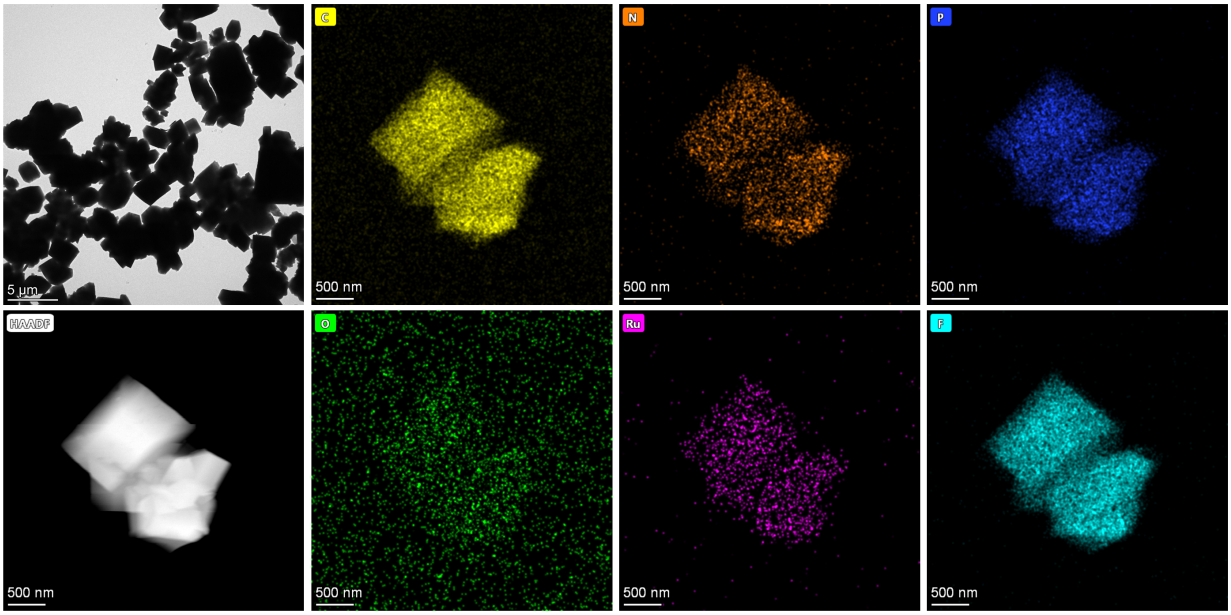

Figure S14. TEM, HAADF and elemental mapping (C-red, N-green, O-blue, P-cyan, F-yellow, Ru-pink) of the **1 µm** $[Ru(bpy)_2(dmbpy)](PF_6)_2$ microparticles prepared by fast precipitation at 0 °C.

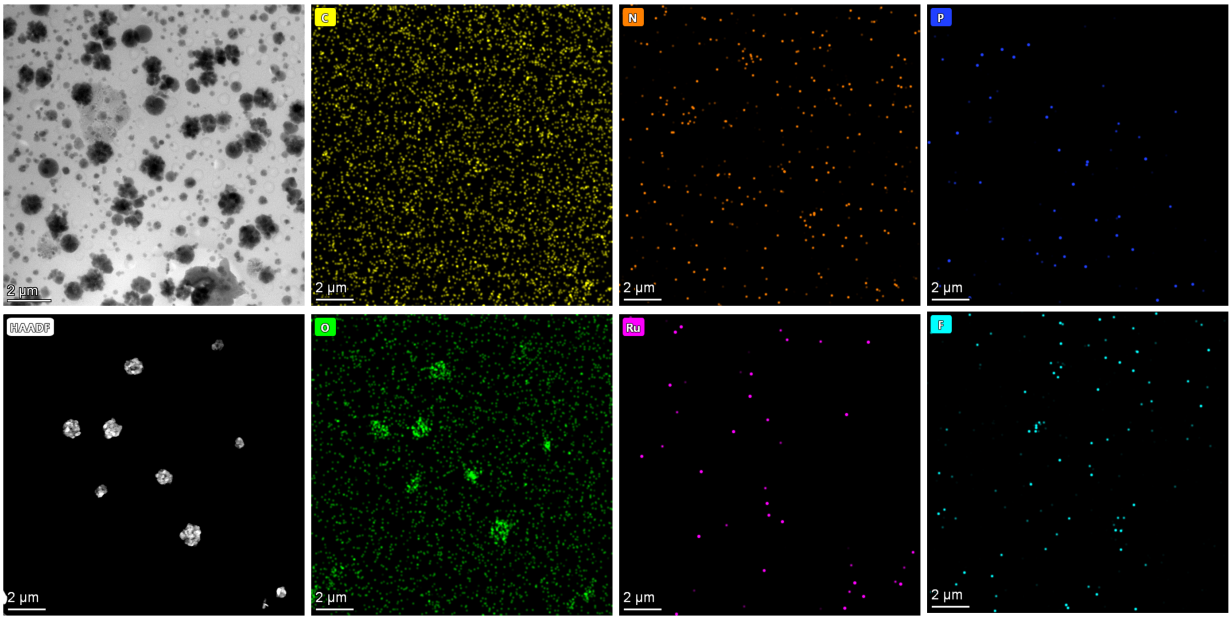

Figure S15. TEM, HAADF and elemental mapping (C-red, N-green, O-blue, P-cyan, F-yellow, Ru-pink) of the **380 nm PVP** $[Ru(bpy)_2(dmbpy)](PF_6)_2$ nanoparticles prepared by fast precipitation at room temperature in the presence of PVP55 confining agent.

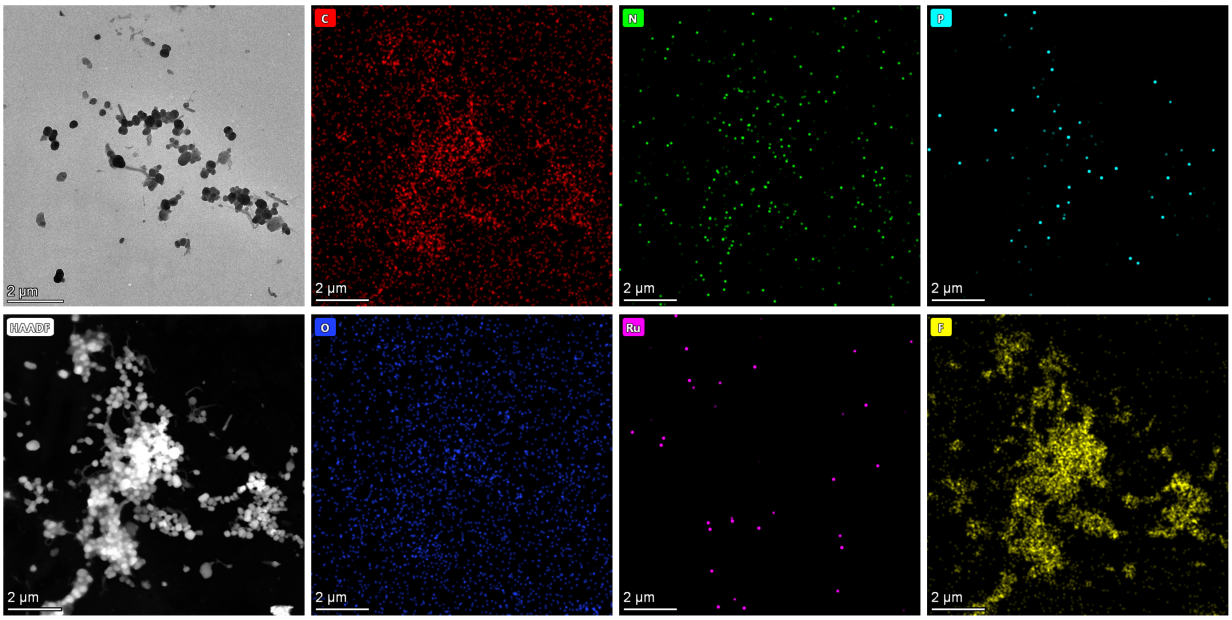

Figure S16. TEM, HAADF and elemental mapping (C-red, N-green, O-blue, P-cyan, F-yellow, Ru-pink) of the **300 nm PEG** $[Ru(bpy)_2(dmbpy)](PF_6)_2$ nanoparticles prepared by fast precipitation at room temperature in the presence of PEG6000 confining agent.

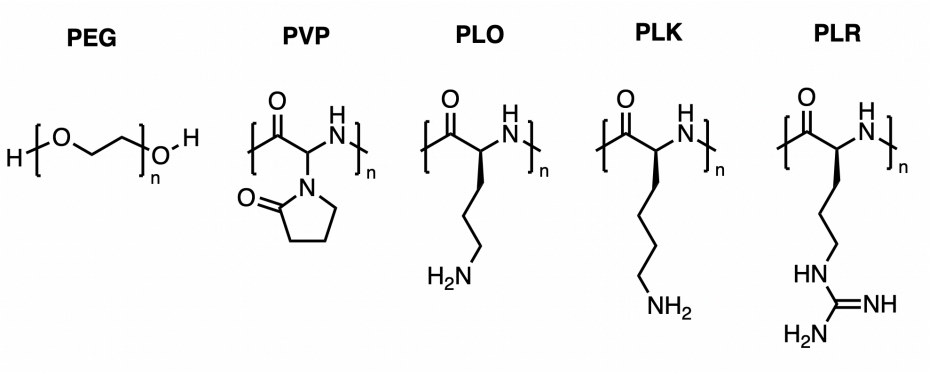

Figure S17. Chemical structures of polymers used in this study. PEG is polyethylene glycol; PVP is polyvinylpyrrolidone; PLO is poly(L-ornithine); PLK is poly(L-lysine); and PLR is poly(L-arginine).

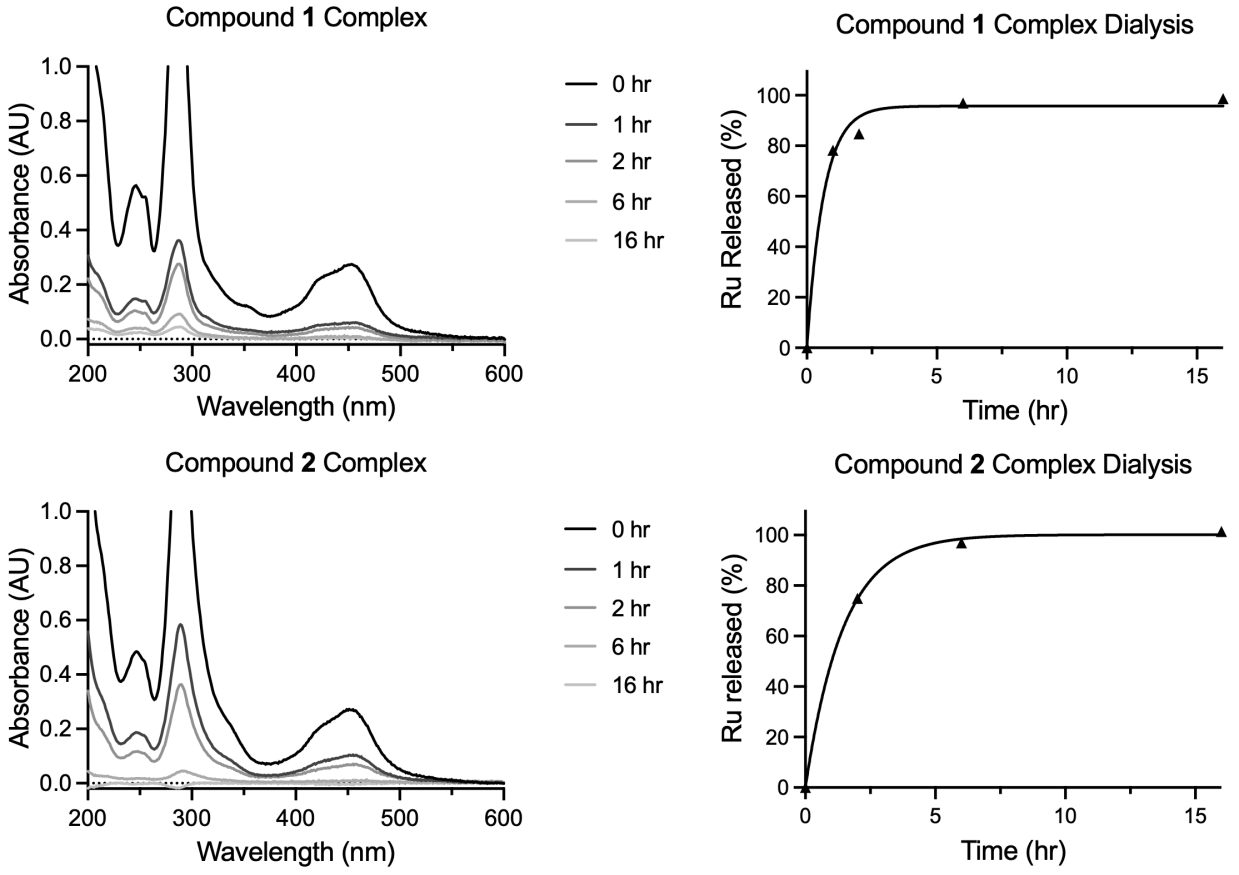

Figure S18. UV-Visible spectra as function of time of $[Ru(bpy)_3](PF_6)_2$ (top) and $[Ru(bpy)_2(dmbpy)](PF_6)_2$ (bottom) solubilized complex in methanol dialyzed in water at 37°C in the dark.

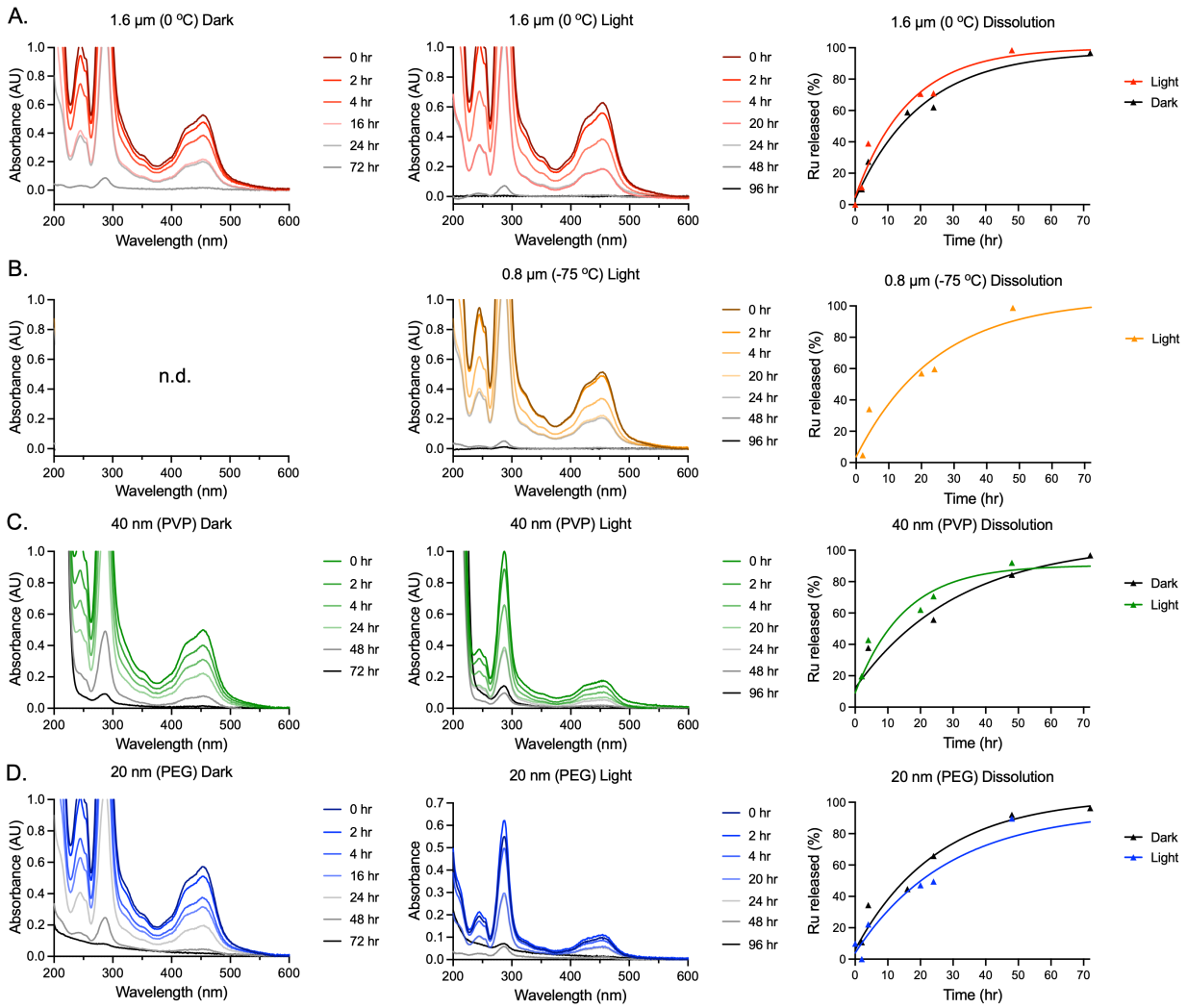

Figure S19. UV-Visible spectra as function of time of $[Ru(bpy)_3](PF_6)_2$ (A) 1.6 µm, (B) 0.8 µm, (C) 40 nm PVP and (D) 20 nm PEG particles PBS suspension (~1 mg/mL) dialyzed in water at 37°C in the dark or after light activation (t = 1min, λ = 450 nm, P = 29.1 J/cm^2) (n.d. = not determined).

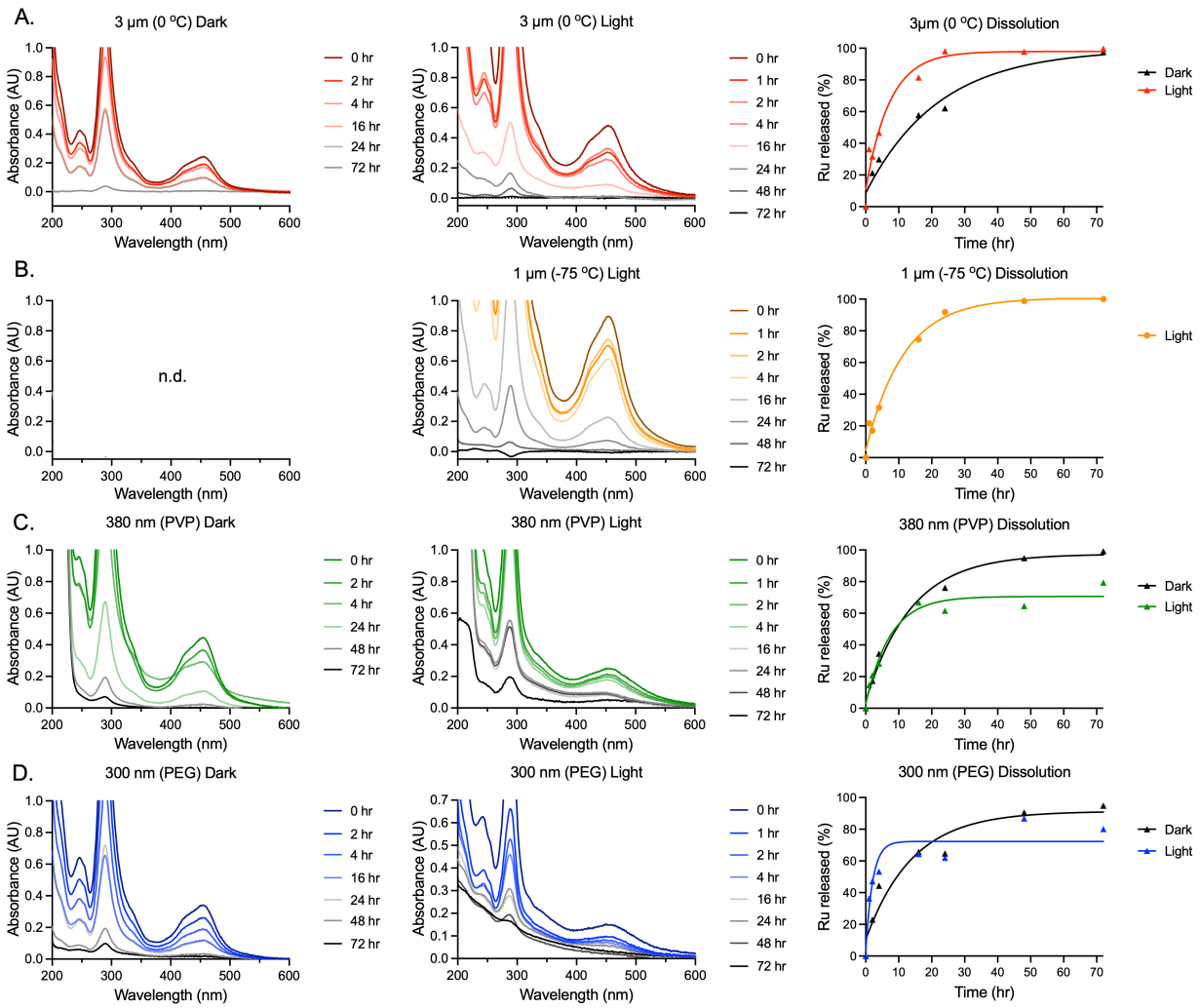

Figure S20. UV-Visible spectra as function of time of $[Ru(bpy)_2(dmbpy)](PF_6)_2$ (A) 3 µm, (B) 1 µm, (C) 380 nm PVP and (D) 300 nm PEG particles PBS suspension (~1 mg/mL) dialyzed in water at 37°C in the dark or after light activation (t = 1min, λ = 450 nm, P = 29.1 J/cm^2) (n.d. = not determined).

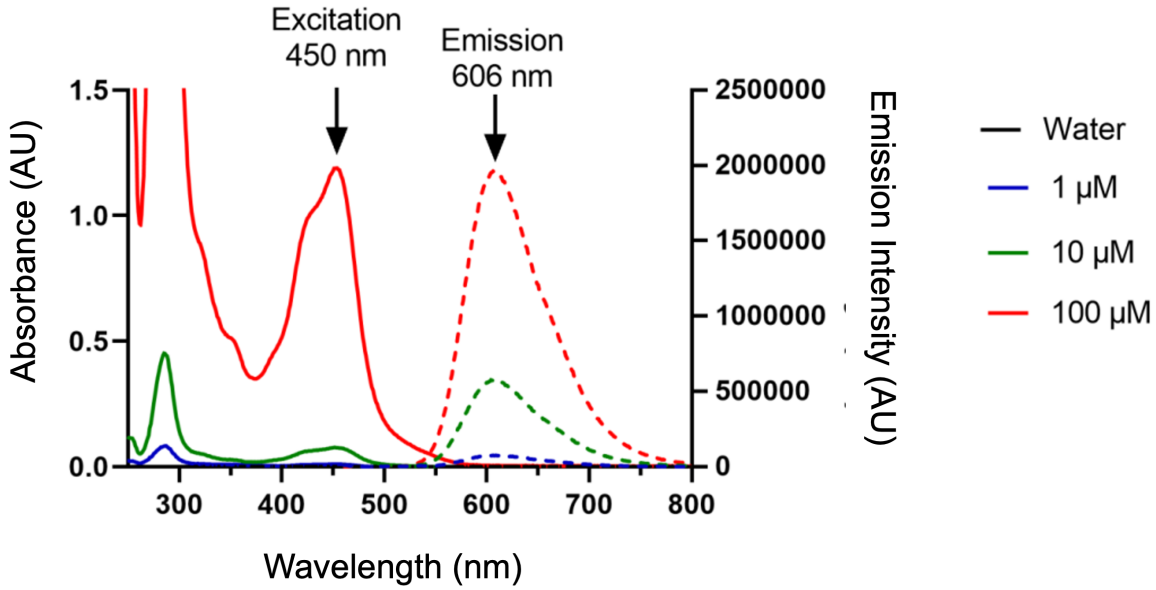

Figure S21. Excitation-emission properties of the $[Ru(bpy)_3)]Cl_2$ complex in water and at different concentration.

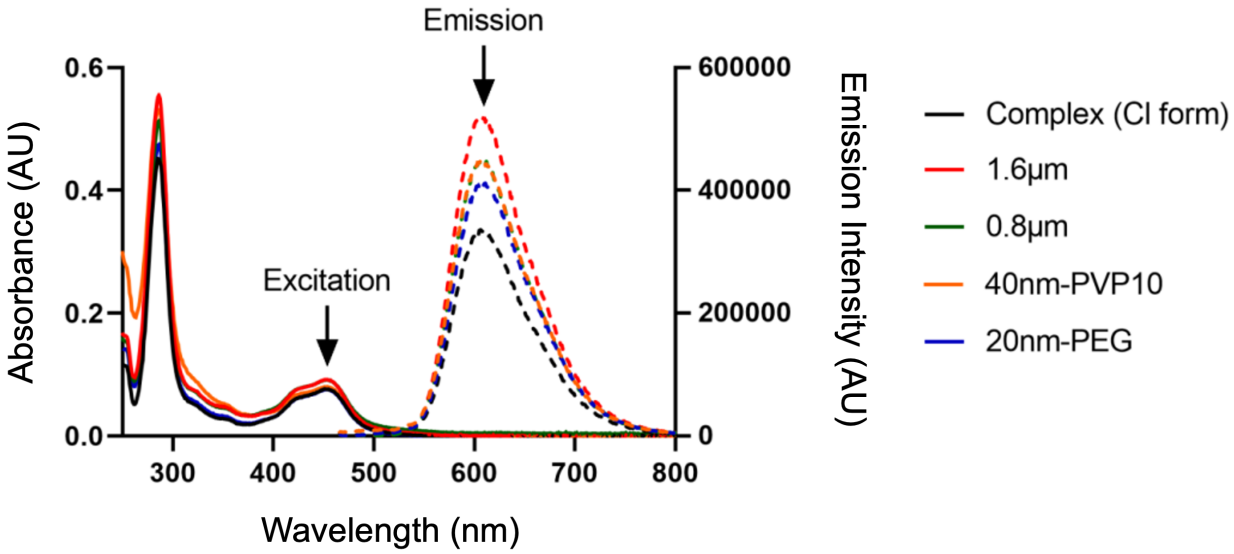

Figure S22. Excitation-emission properties of the $[Ru(bpy)_3](PF_6)_2$ particles compared to the solubilized complex (Cl form) in water (10 µM suspensions).

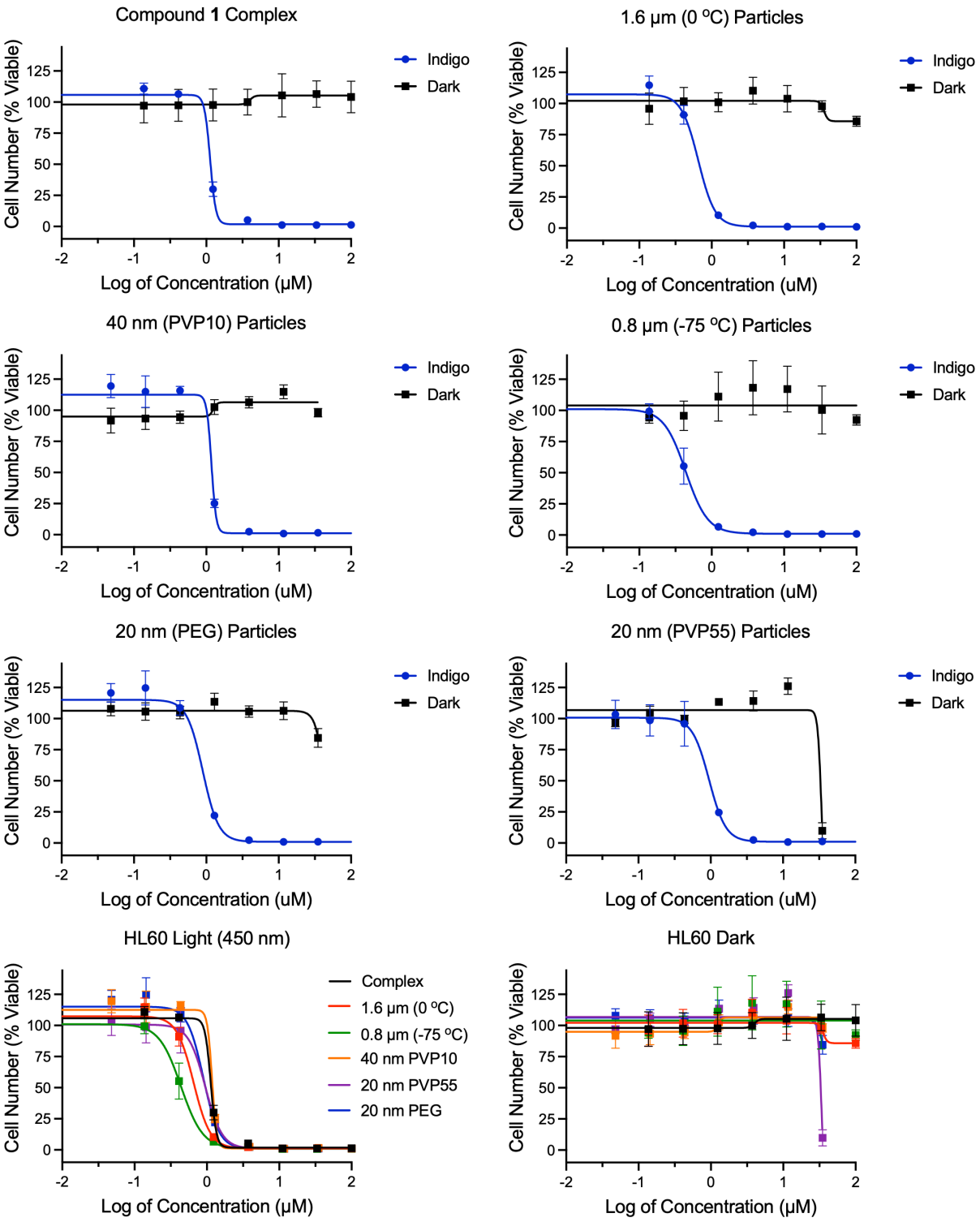

Figure S23. Cytotoxicity dose responses of compound **1** and associated particles in HL60 cells.

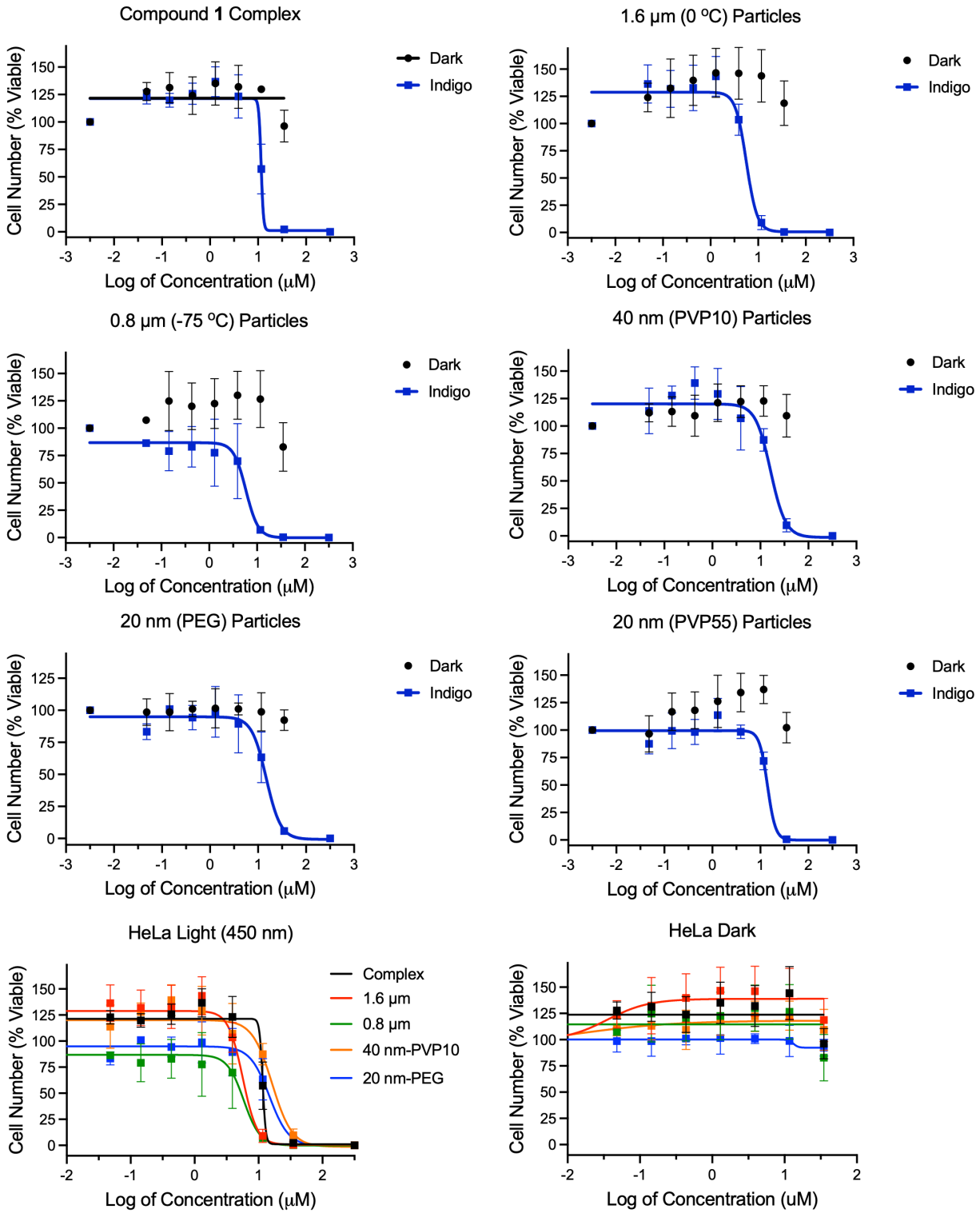

Figure S24. Cytotoxicity dose responses of compound **1** and associated particles in HeLa cells.

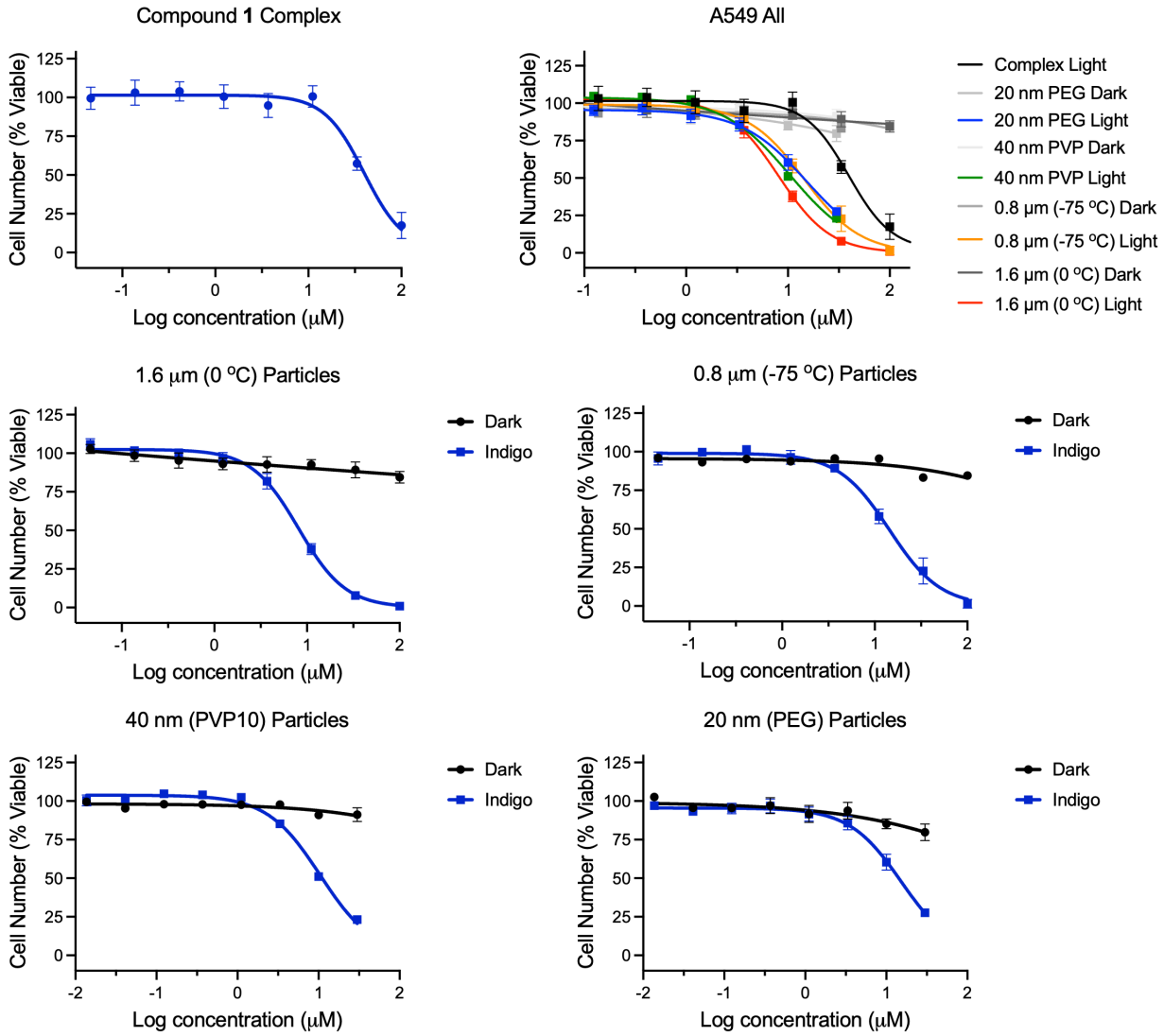

Figure S25. Cytotoxicity dose responses of compound **1** and associated particles in A549 cells.

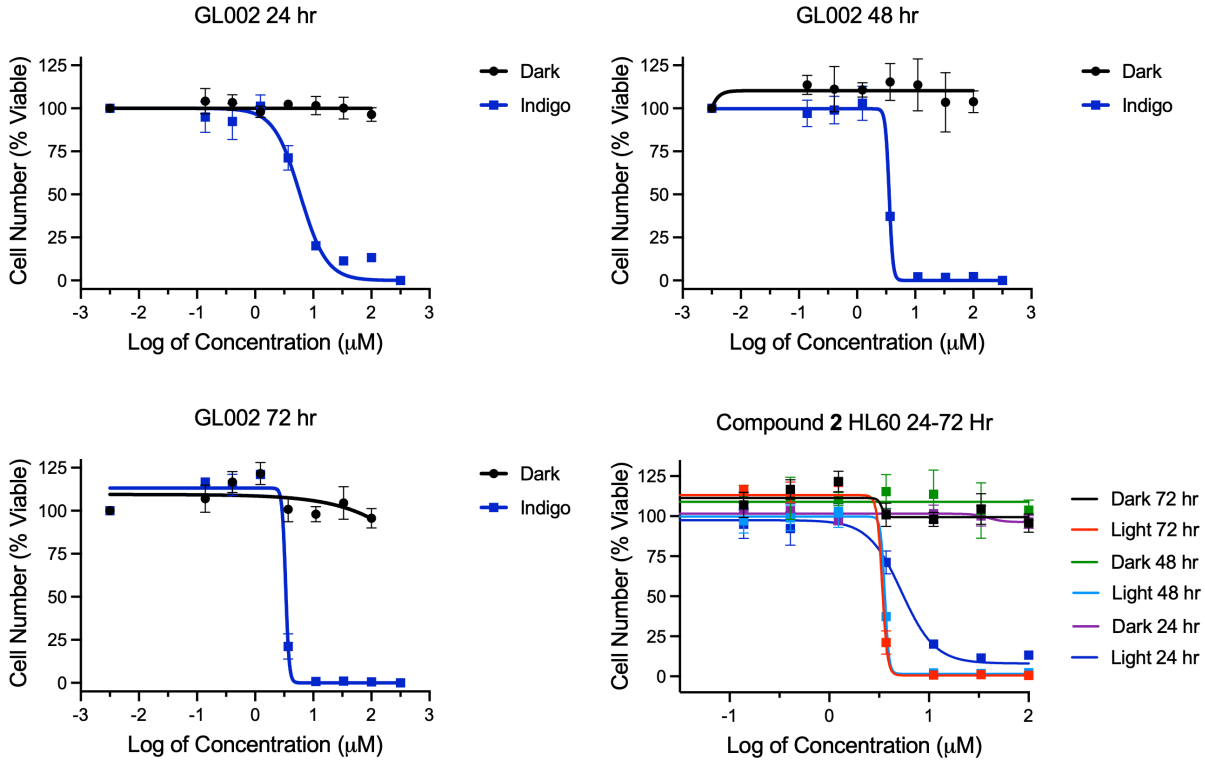

Figure S26. Cytotoxicity dose responses of compound **2** soluble complex with 24, 48, and 72 hour incubation following indigo light irradiation for 1 minute in HL60 cells.

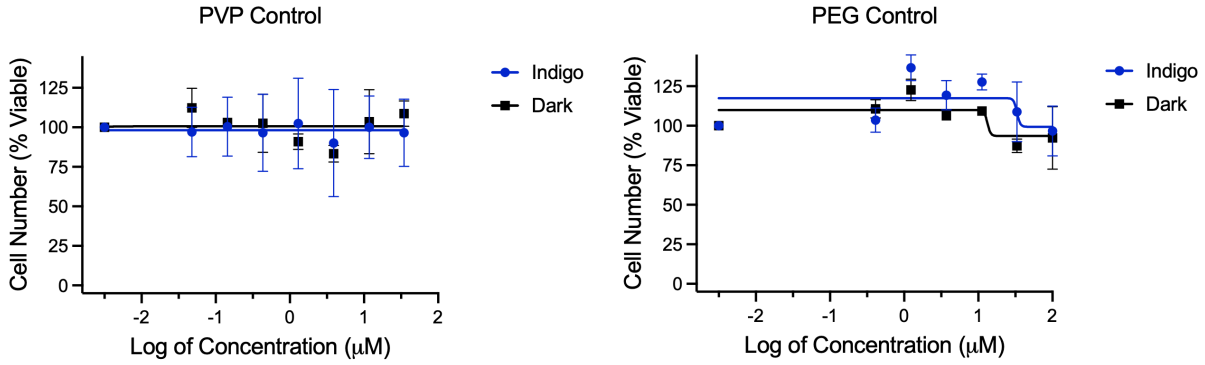

Figure S27. Cell viability of HL60 cells treated with PVP and PEG polymers.

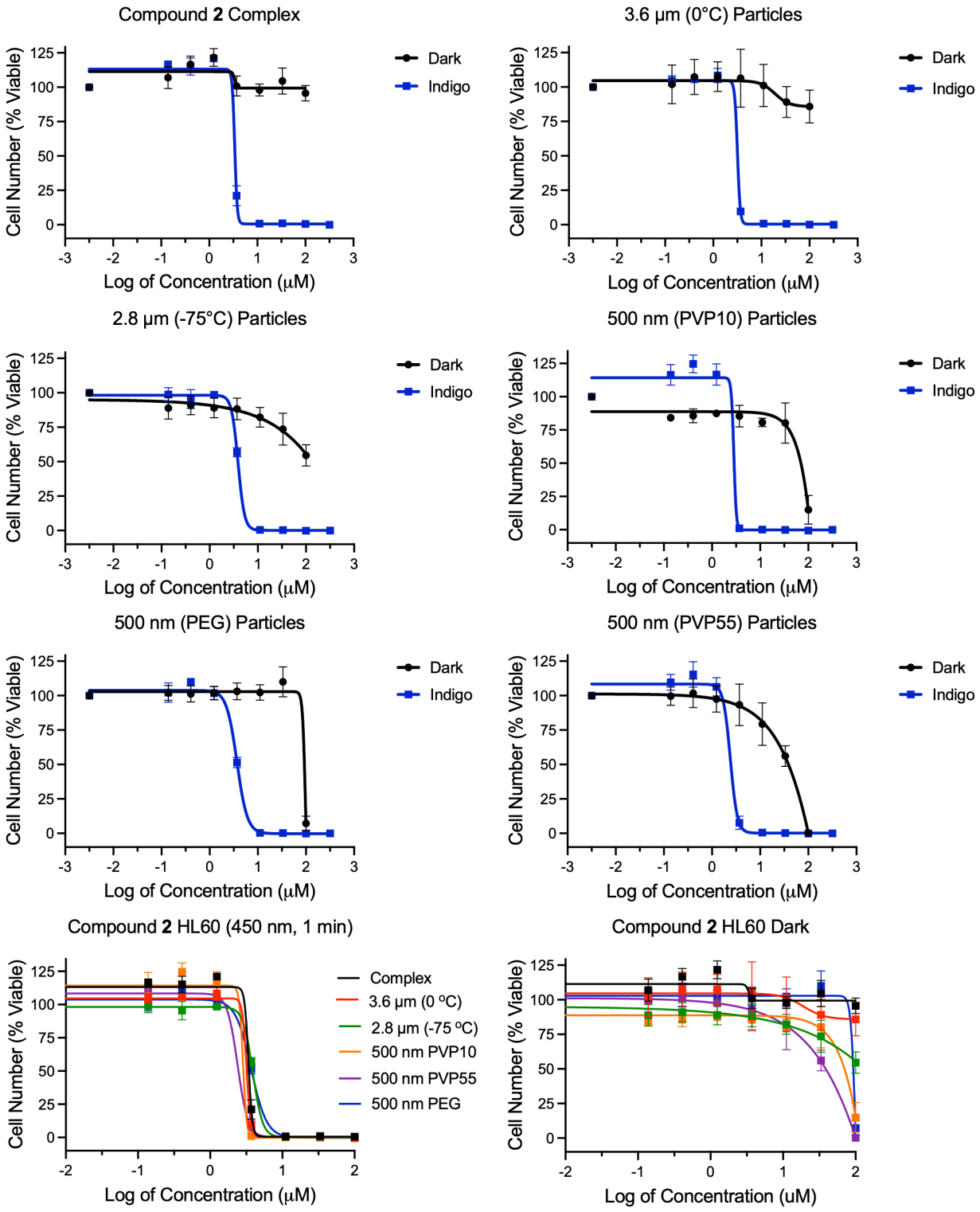

Figure S28. Cytotoxicity dose responses of compound **2** PF_6 and associated particles in HL60 cells.

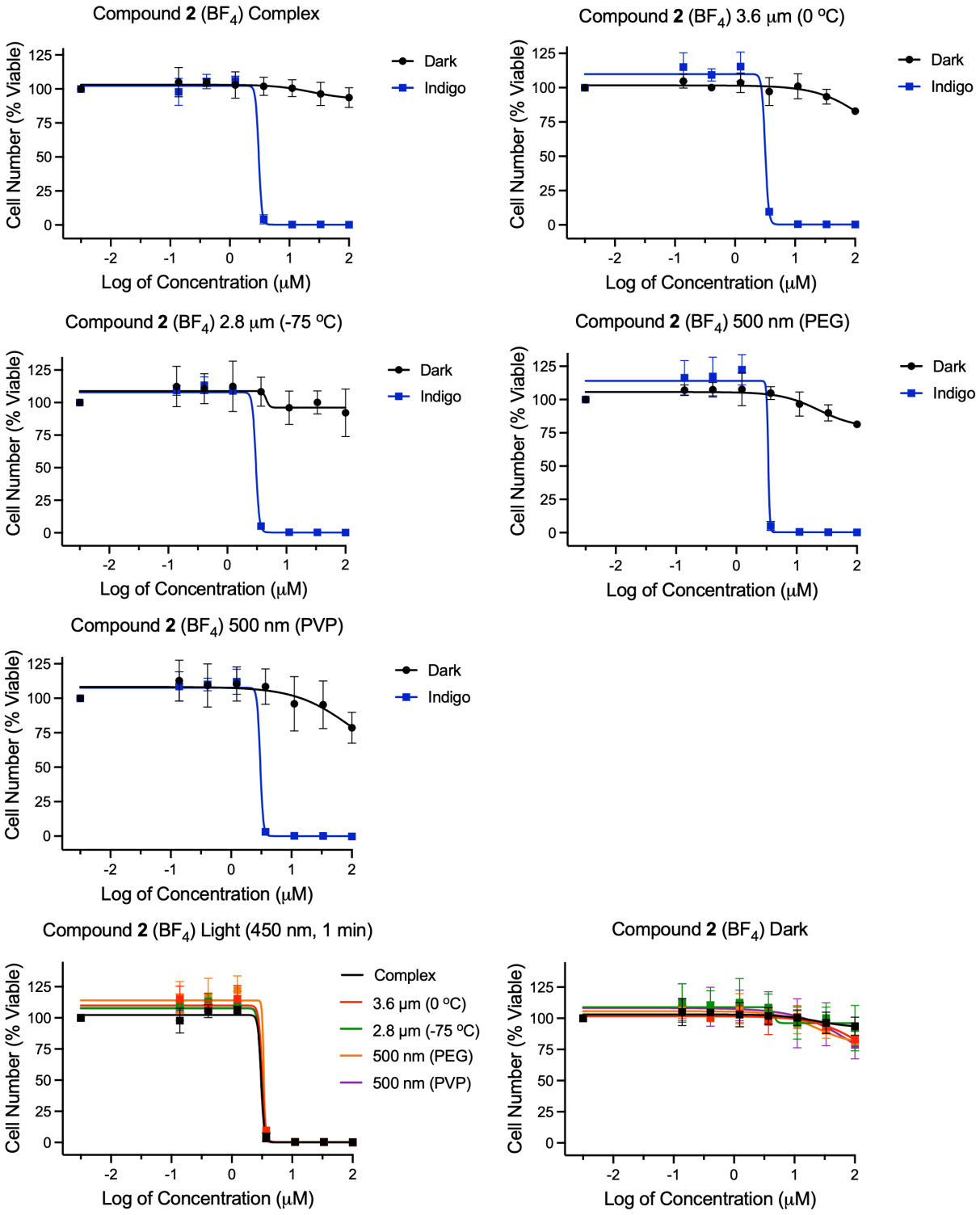

Figure S29. Cytotoxicity dose responses of compound **2** BF_4 and associated particles in HL60 cells.

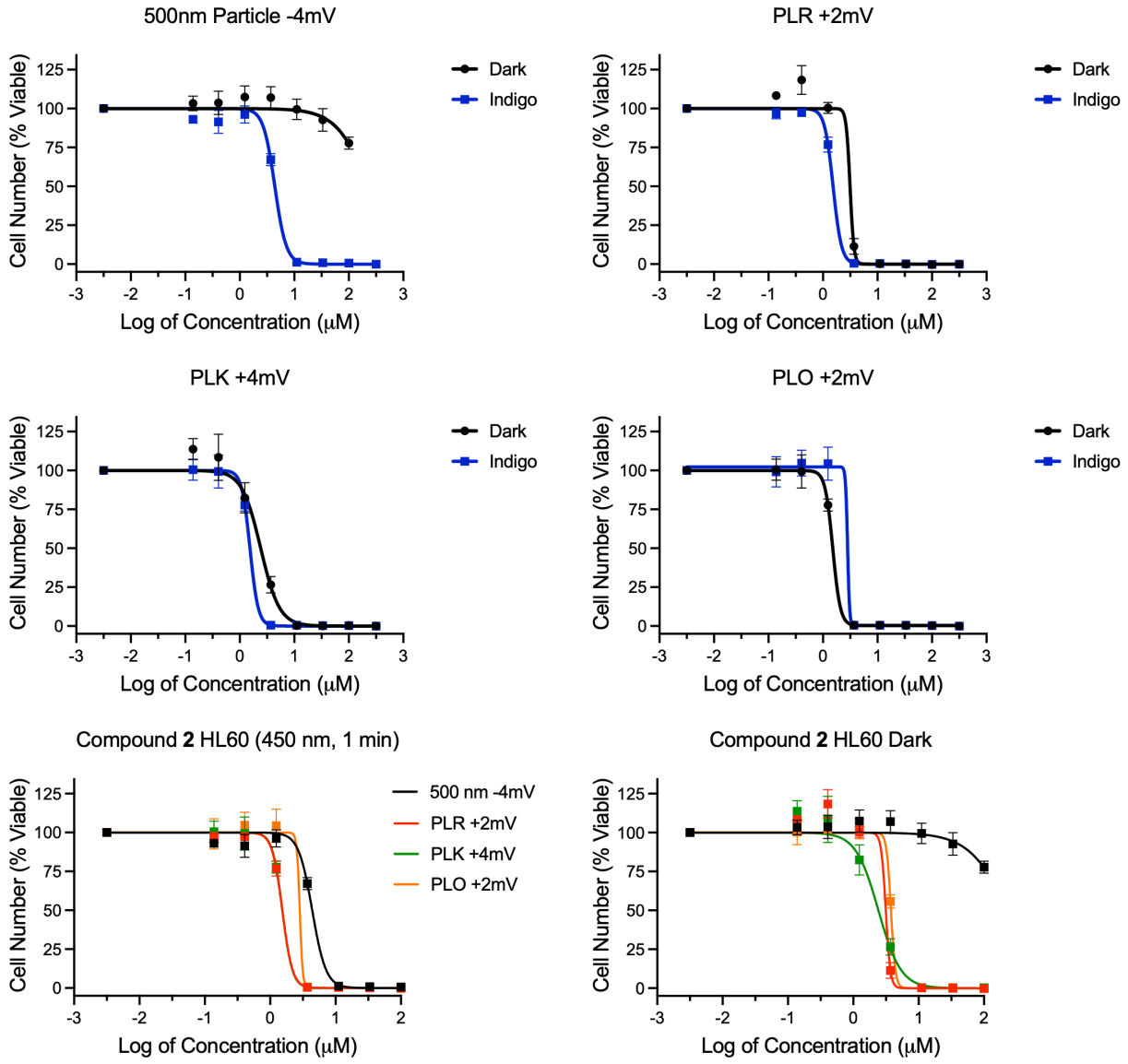

Figure S30. Cytotoxicity dose responses of **500 nm** compound **2** post-functionalized with positively charge PLR, PLK, and PLO polymer in HL60 cells. The measures zeta potentials for 500 nm particles prepared with PLR, PLK, and PLO were +2 mV, +4 mV, and +2 mV, respectively. The uncoated 500 nm particles had a zeta potential of -4 mV, consistent with previous preparations.

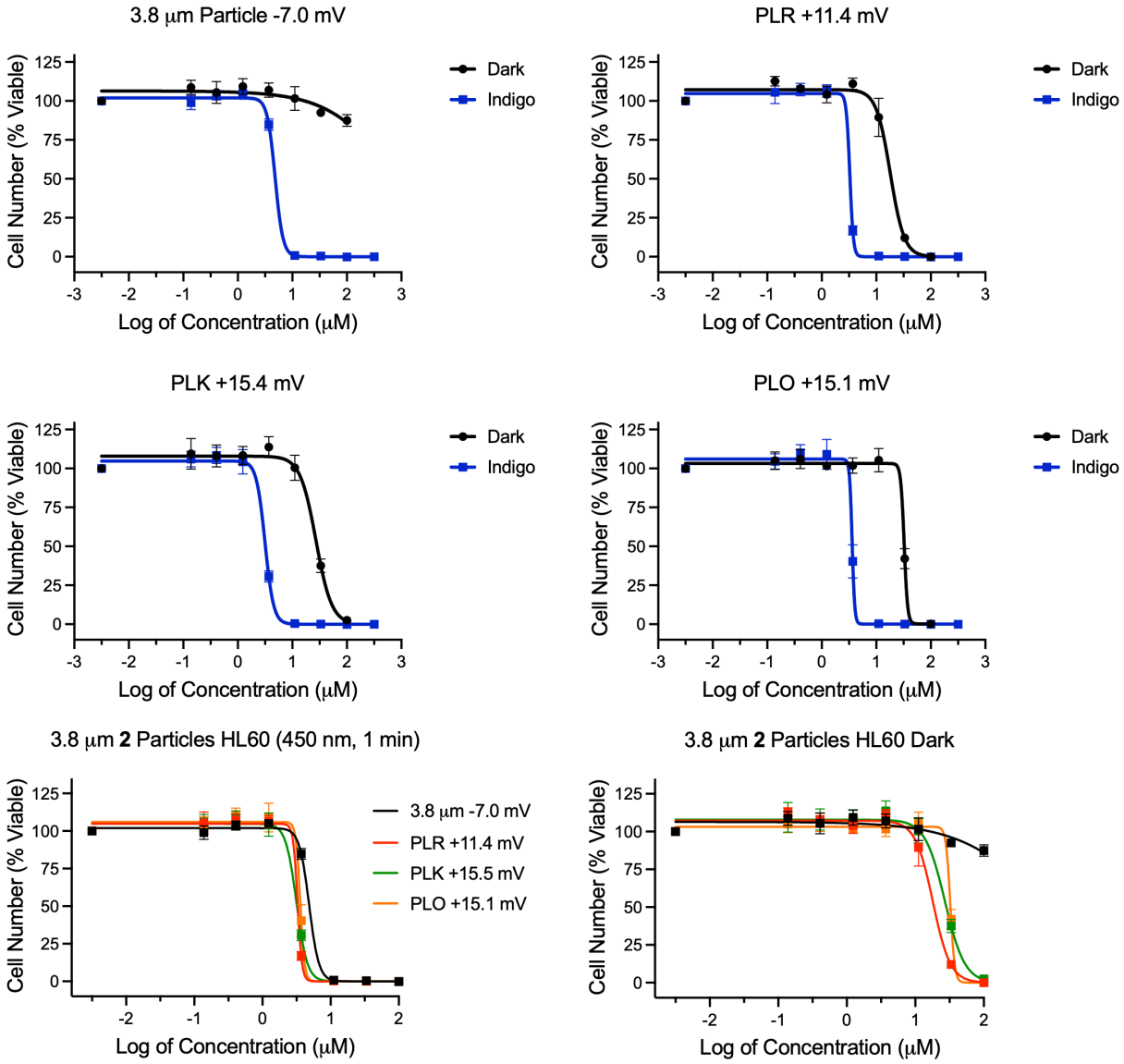

Figure S31. Cytotoxicity dose responses of **3.8 μm** compound **2** post-functionalized with positively charge PLR, PLK, and PLO polymer in HL60 cells. The measures zeta potentials for 3.8 μm particles prepared with PLR, PLK, and PLO were +11.4 mV, +15.4 mV, and +15.1 mV, respectively. The uncoated 3.8 μm particles had a zeta potential of -7 mV, consistent with previous preparations.

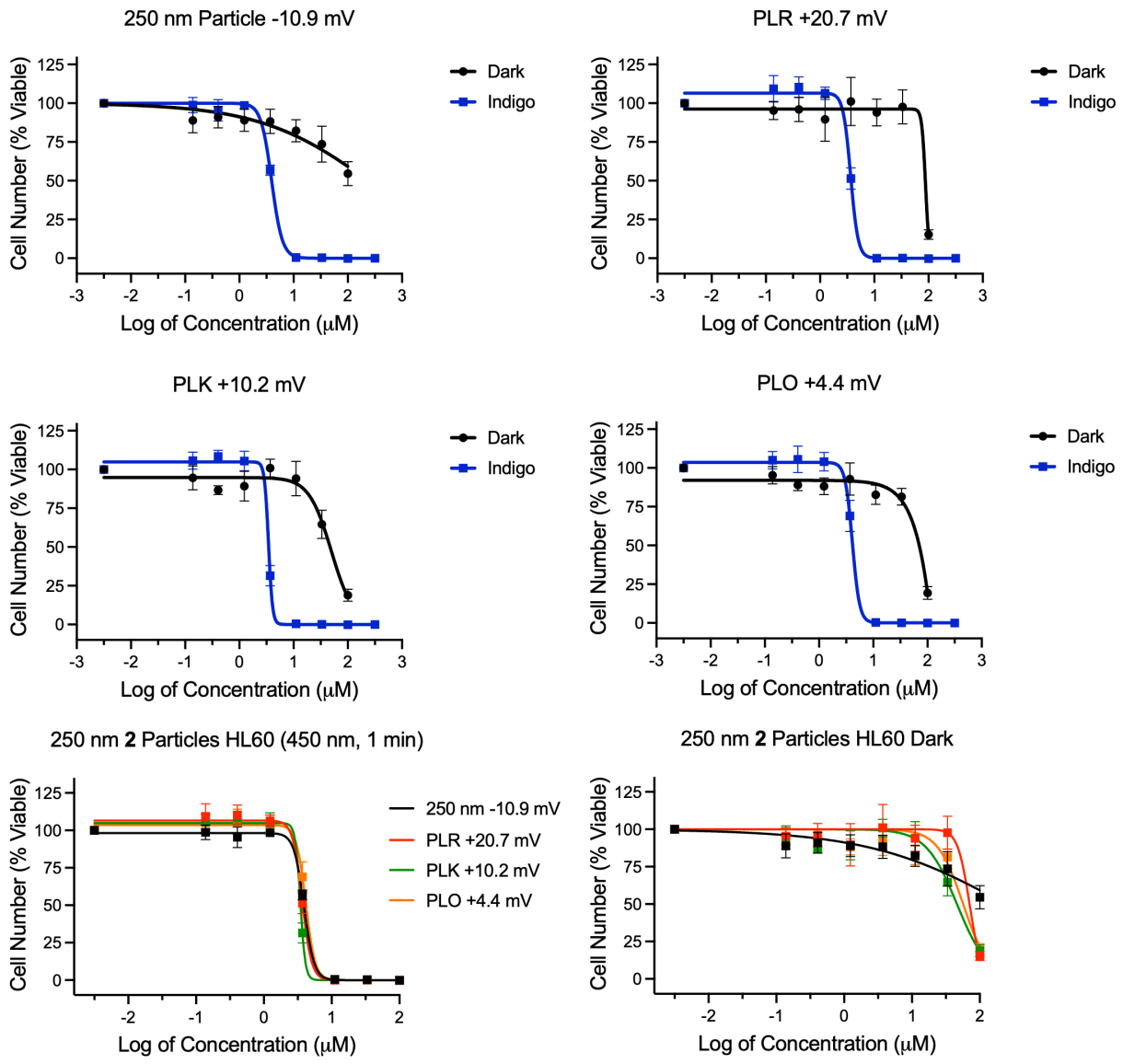

Figure S32. Cytotoxicity dose responses of **250 nm** compound **2** post-functionalized with positively charge PLR, PLK, and PLO polymer in HL60 cells. The measures zeta potentials for 250 nm particles prepared with PLR, PLK, and PLO were +20.7 mV, +10.2 mV, and +4.4 mV, respectively. The uncoated 250 nm particles had a zeta potential of -10.9 mV, consistent with previous preparations.

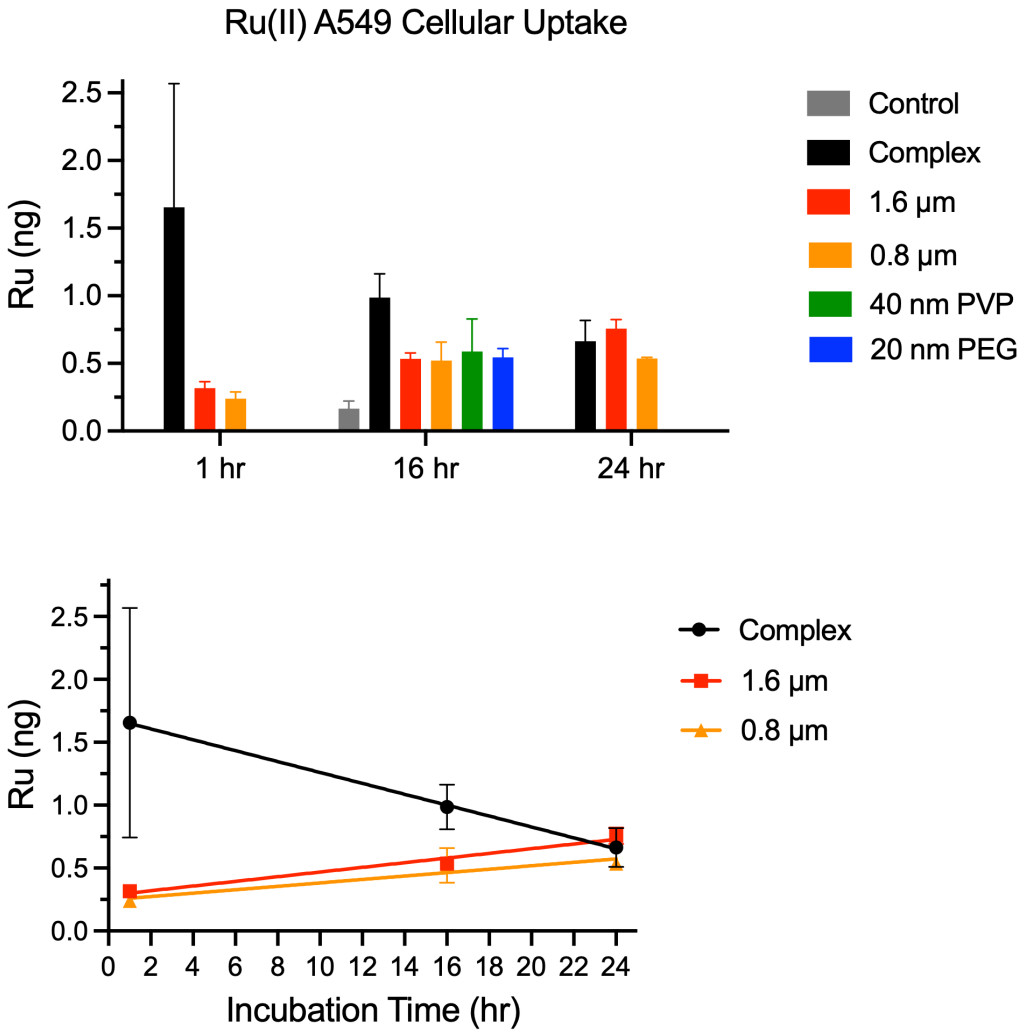

Figure S33. Accumulation of Ru in A459 cells at 1, 16, and 24 hours for compound **1** and associated particles (top) and the change in intracellular Ru content over time fitted with a linear regression (bottom).

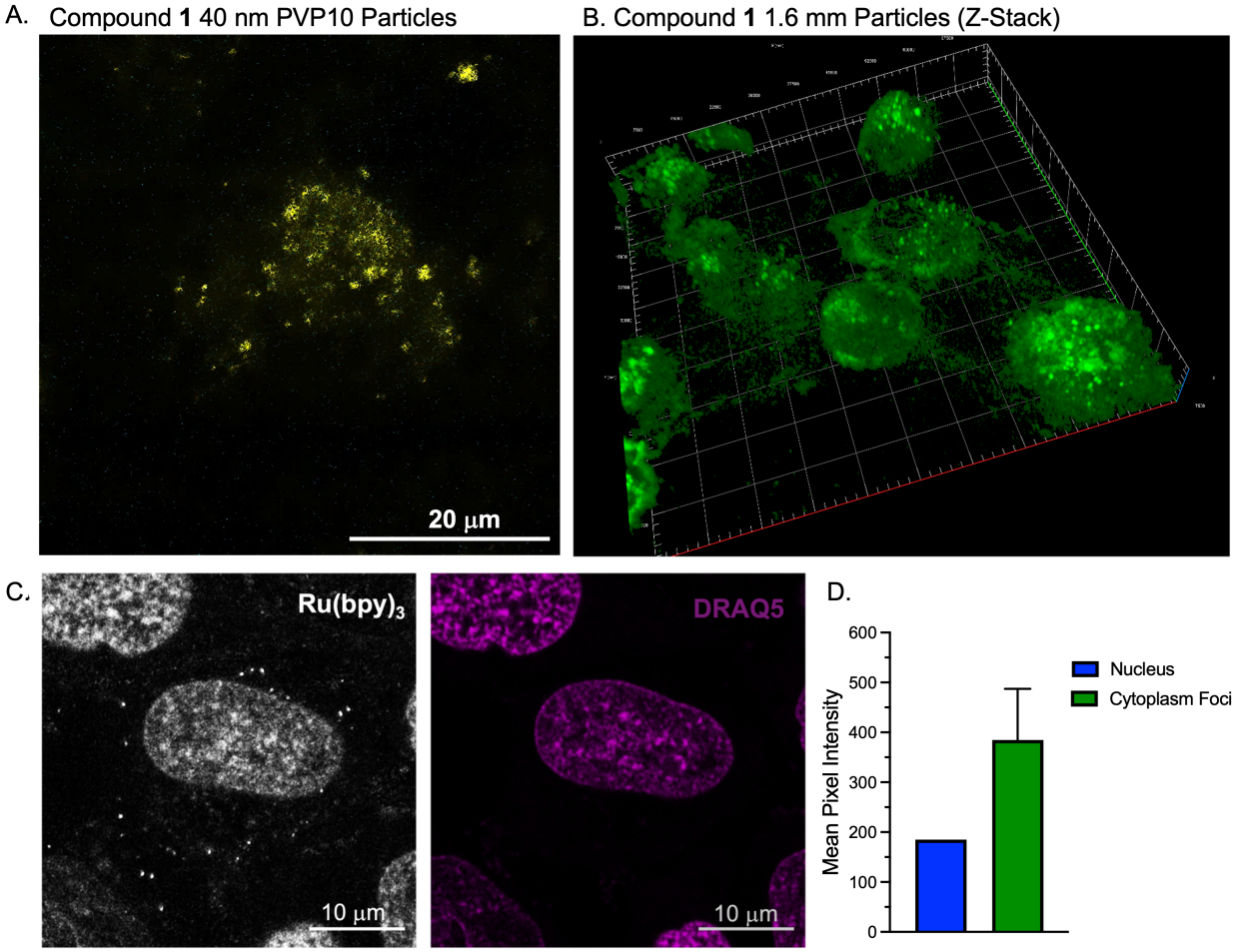

Figure S34. Fluorescence localization microscopy of compound **1** particles. (A) 40 nm PVP10 nanoparticles and released complex; (B) z-stack 3D rendering of 1.6 mm particles; (C) single plane image of 1.6 mm particles microparticles and released complex (left) and DRAQ5 nuclear stain (right); (D) plot of mean pixel intensity of $Ru(bpy)_3$ signal in the nucleus versus foci located in the cytoplasm.

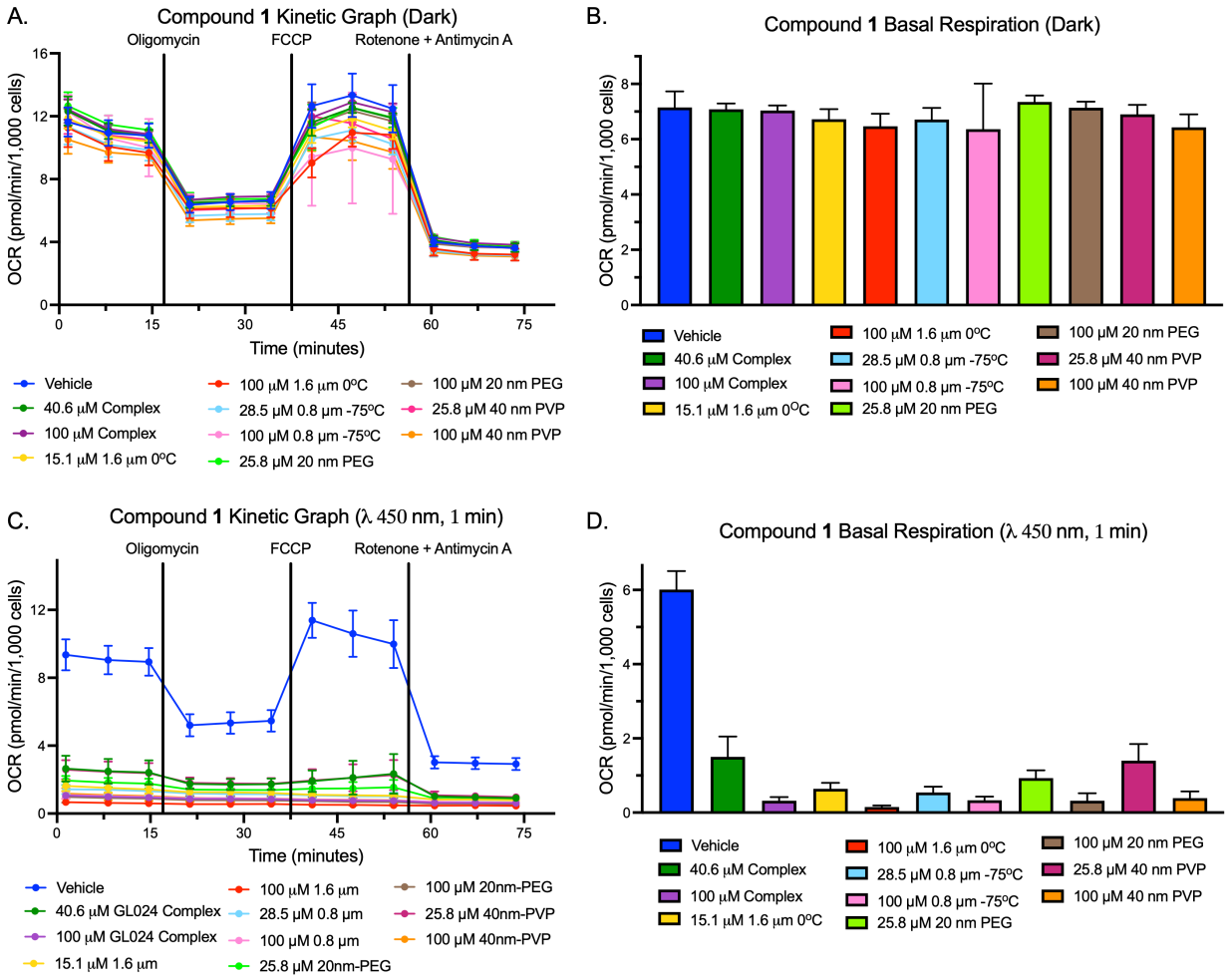

Figure S35. Seahorse extracellular flux analysis and basal respiration of compound **1** (A-B) in the absence of light and (C-D) with 1 minute indigo light irradiation.

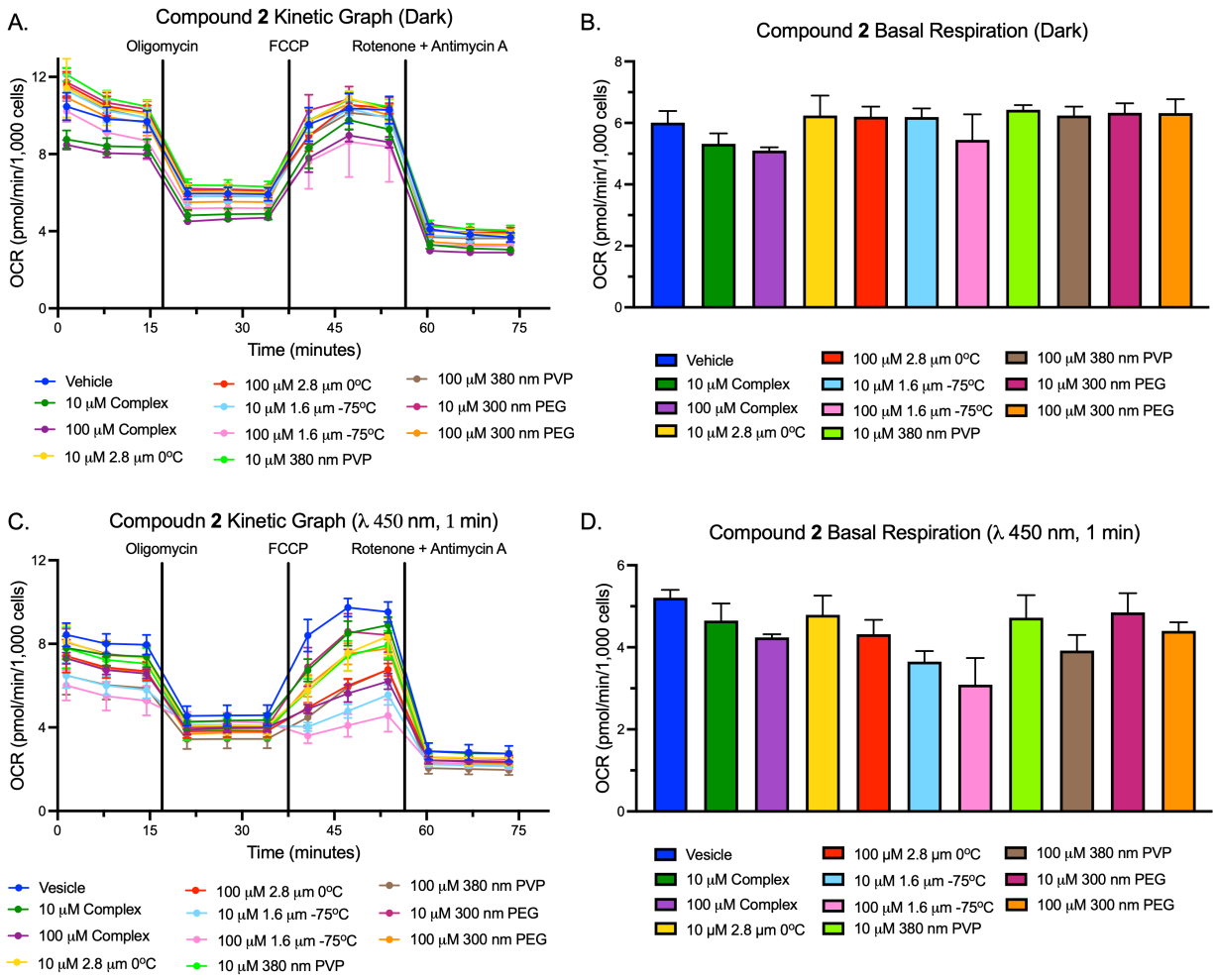

Figure S36. Seahorse extracellular flux analysis and basal respiration of compound **2** (A-B) in the absence of light and (C-D) with 1 minute indigo light irradiation.

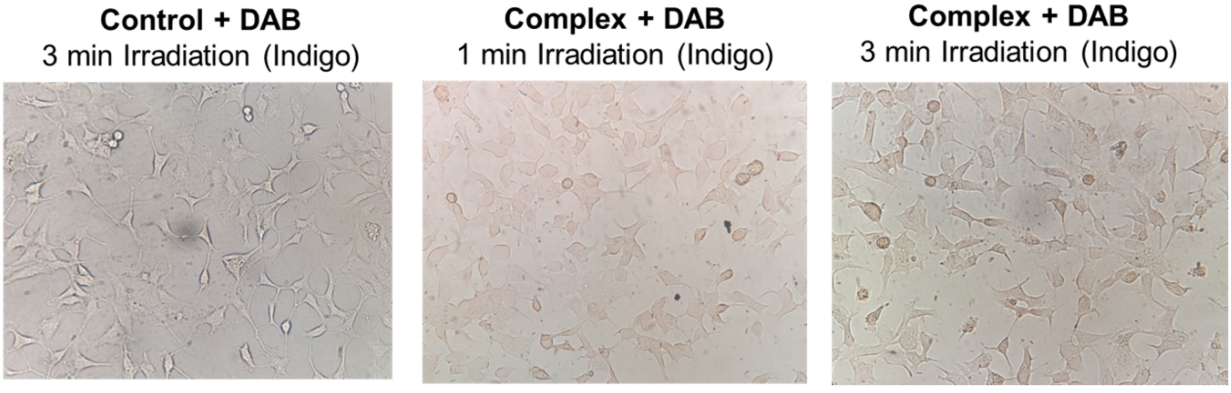

Figure S37. DAB polymerization in A459 cells followed by light microscopy as function of the irradiation time in presence of the $[Ru(bpy)_3](PF_6)_2$ complex.

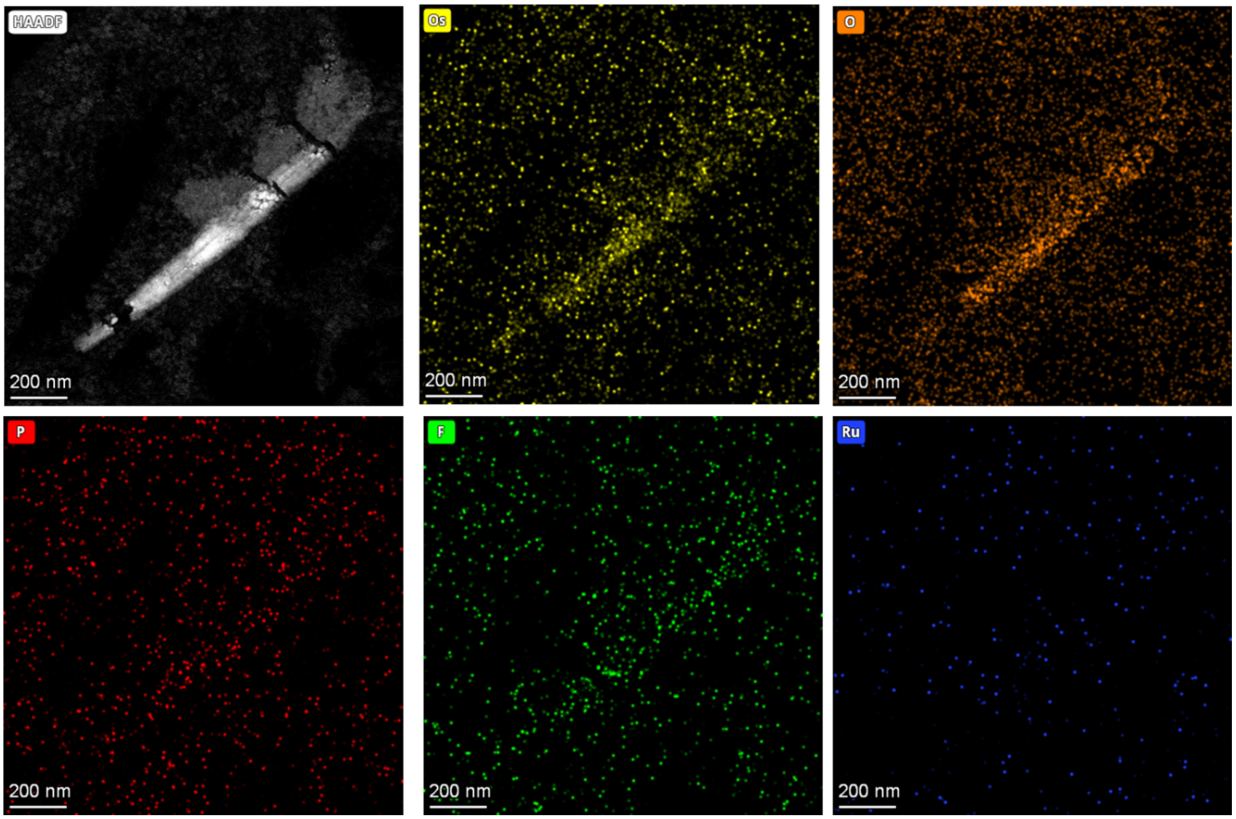

Figure S38. TEM, HAADF and EDS mapping (Os, O, P, F, Ru) of a 1.6 µm particle undergoing dissolution in A459 cells.

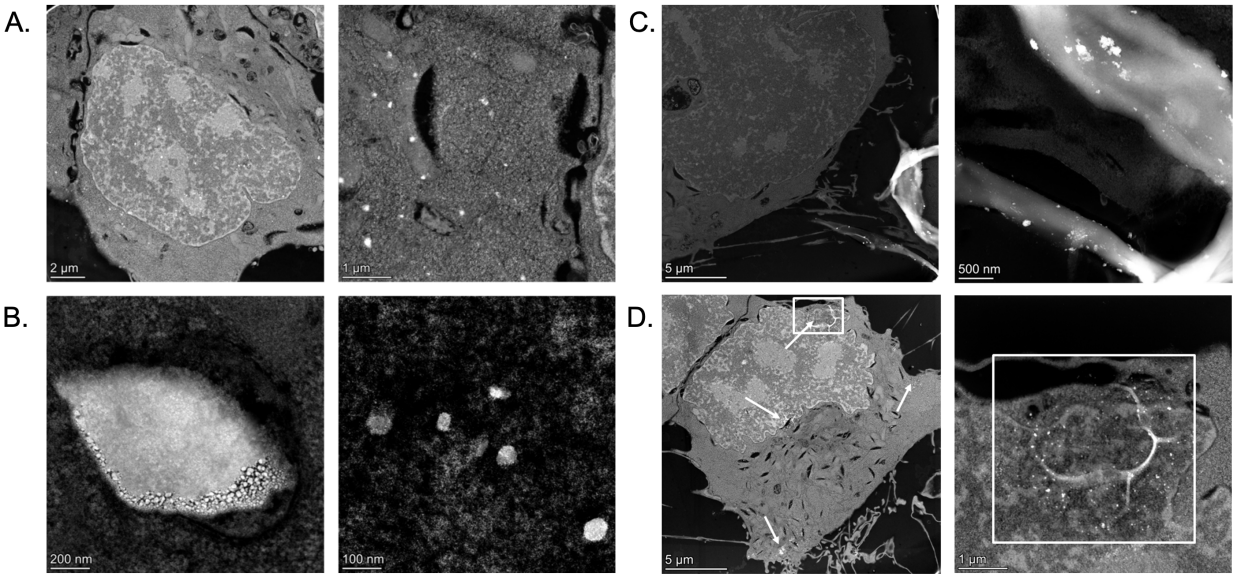

Figure S39. STEM images of A549 cells cross sections treated with compound 1 soluble complex and 40 nm PVP particles. (A) DAB deposit found in nucleus and cytosol, (B) dissolution

process of aggregate into small particles, (C) 40 nm particles of 1 embedded in PVP biodegradable film, (D) release of the nanoparticles in the cytosol and nucleus.

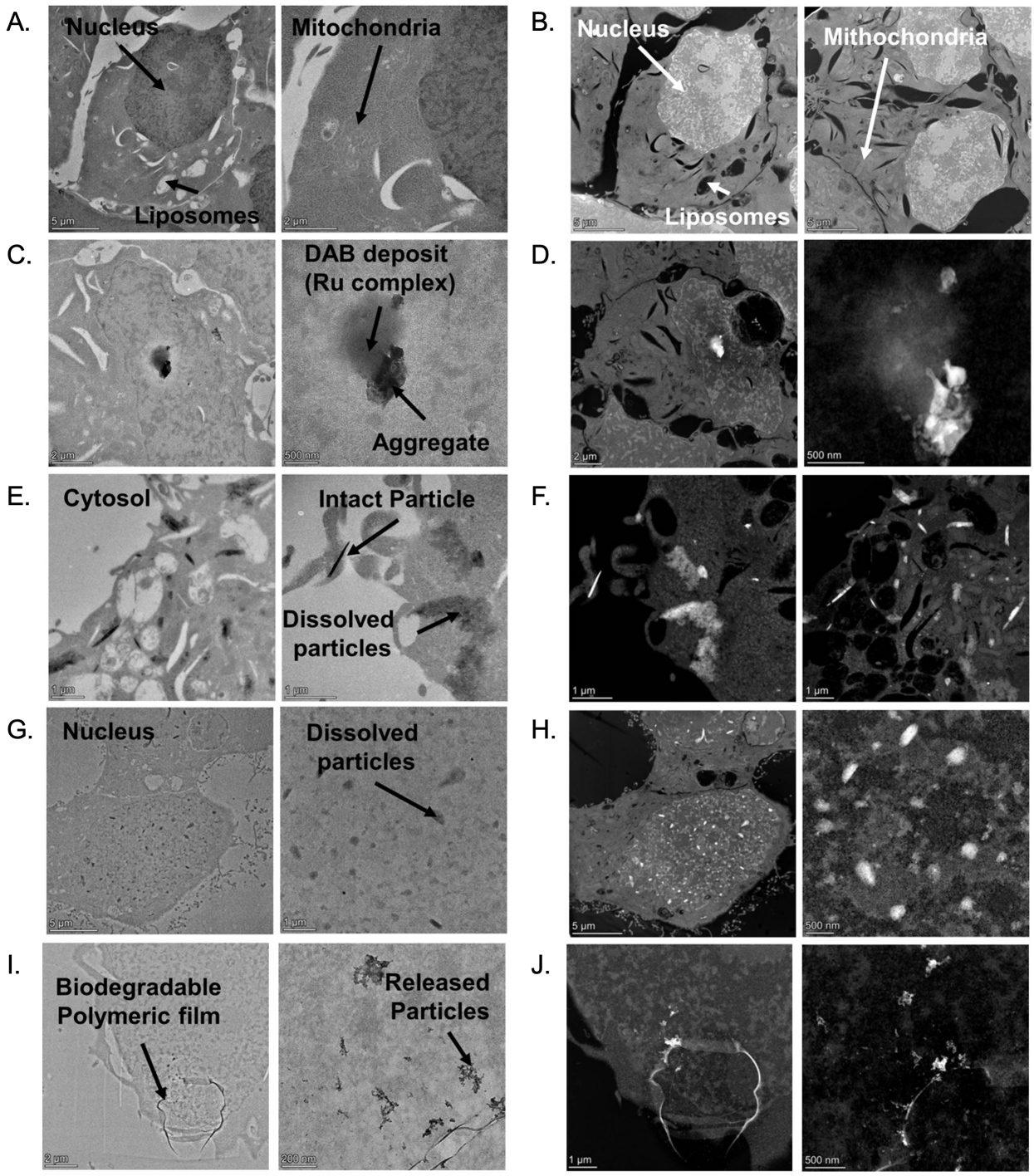

Figure S40. TEM (left) and STEM (right) images of A459 cell cross sections for cells (A-B) untreated or treated with 20 μM of (C-D) compound **1**, (E-H) 1.6 μm particles and (I-J) 40 nm PVP particles for 16 hours.

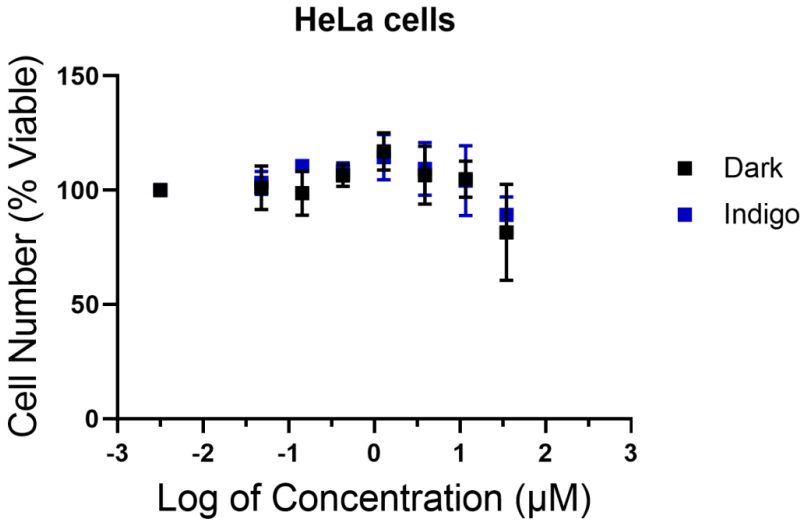

Figure S41. HeLa cells viability after incubation for 72h in the dark or after irradiation (Indigo light) for 1 min with $[Ru(bpy)_2(dmbpy)](PF_6)_2$ complex.

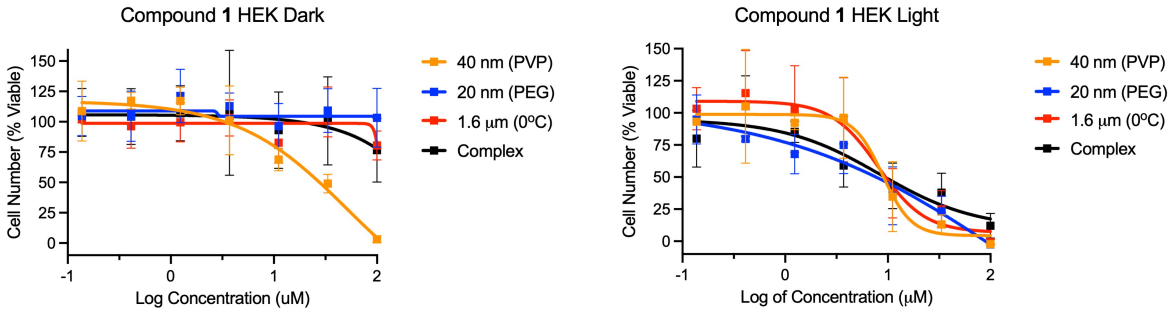

Figure S42. Cytotoxicity dose responses of compound **1** and associated particles in HEK cells. Samples were either protected from light for the dark condition or exposed to indigo light for 1 minute (t = 1min, λ = 450 nm, P = 29.1 J/cm^2).